7-23-2019

Functional porous polydimethlysiloxane as piezoresistive and piezoelectric materials

Taissa Rose Michel
Rowan University

FUNCTIONAL POROUS POLYDIMETHYLSILOXANE AS PIEZORESISTIVE AND PIEZOELECTRIC MATERIALS

by

Taissa Rose Michel

A Thesis

Submitted to the
Department of Mechanical Engineering
In partial fulfillment of the requirement
For the degree of
Master of Science in Mechanical Engineering
at
Rowan University
May 17, 2019

Thesis Advisor: Wei Xue, Ph.D

Dedications

A special thanks to everyone who has helped me along this journey. To my inspiring father, John Michel, thank you for all your support and encouragement. To my loving fiancé, Joseph Nalbach, thank you for always being there with a helping hand.

Acknowledgments

I would like to give special acknowledgments to my advisor, Dr. Wei Xue. Thank you for all your guidance both during my undergraduate and graduate studies. I would also like to recognize Dr. Kadlowec and Dr. Bakrania for being a part of my defense committee. Both of you have been so important to me as I grew into a Rowan University engineer. Thank you all for everything you have done for me as teachers, mentors, and friends.

To my wonderful lab mates and friends, Christian Beauvais, Harrison Hones, Matthew Schwenger, Muhammad Usman, Medhi Benmassaoud, and Joseph Ianello, thank you for sharing your ideas, your ambitions, and most importantly, your laughs with me.

Abstract

Taissa Rose Michel
FUNCTIONAL POROUS POLYDIMETHYLSILOXANE AS PIEZORESISTIVE AND PIEZOELECTRIC MATERIALS
2018-2019
Wei Xue, Ph.D.
Master of Science in Mechanical Engineering

In this paper, polydimethylsiloxane (PDMS), carbon nanotubes (CNTs), and zinc oxide (ZnO) were combined to create functionalized piezoresistive and piezoelectric sensors for pressure sensing and energy harvesting. Samples were foamed to show that the increased deformability of the foam sensors makes them suitable for a range of applications including dexterous robotics, tactile sensing, energy harvesting, and biosensing. Uniform dispersion of CNTs was achieved with chloroform as the solvent. Samples were foamed using chemical blowing and scaffolding but granulated sugar at 70% porosity resulted in foamed samples with the most consistent mechanical properties. Samples underwent tensile and compressive testing for their mechanical properties. These test's results showed that introducing pores did not significantly degrade sensor performance. Porous devices are more ductile and use less materials than their bulk counterparts. Piezoresistive sensors with 3.5% CNTs yielded the highest sensitivity with a Young's modulus of 0.42 MPa. To further functionalize the devices, ZnO is mixed into the samples to produce piezoelectric devices. Dipole alignment is done in an attempt to increase the output power of piezoelectric devices. This resulted in a 5× increase in performance of the devices and further research needs to be conducted. Overall, porous PDMS functions for both piezoelectric and piezoresistive device applications.

Table of Contents

Table of Contents (Continued)

Table of Contents (Continued)

Table of Contents (Continued)

List of Figures

List of Figures (Continued)

List of Figures (Continued)

List of Figures (Continued)

List of Figures (Continued)

List of Tables

Chapter 1

Introduction

1.1. Sensors

In today's modern technological world, sensors have a variety of functions and applications. The pursuit of knowledge has led to a profusion of developments for sensor technology over the last decade and even spanning into earlier years [1]. Sensors can be used to measure and quantify metrics about the physical world around them; tactile data, velocity, acceleration, water pressure, volumetric flow rates, altitude, electrical output, and many other attributes can be quantified using sensors that have been and are being developed in research labs around to globe.

Often, sensors rely on microelectromechanical systems (MEMS) in order to gather data on the world around them. This development stems mostly from the advances in semiconductor technologies beginning in the 1970's and continuing onward. From this, devices such as inkjet printers, metal-oxide-semiconductors (MOS) sensors, and other increasingly accurate accelerometers have been developed. These devices have been produced for the commercial market in the years after they were invented [2]. Consequentially, wearable electronics for application in biosensing and energy harvesting have been developed using some similar technologies [3]. However, these devices are limited both in their performance and in the lifetime of their power source, a hurdle that researchers must work through. With the aid of nanocomposites and nanomaterials, such a device could be fabricated [4].

Nanocomposite devices can be functionalized to perform any number of sensing tasks. A very common and well researched application is tactile sensing. Many MEMS tactile sensors, though, are limited in that their brittleness restricts both overall flexibility

and long-term performance. The degree to which a device can stretch and/or flex is very important for tactile sensors for robotic hands or manipulators. These applications require a high degree of flexibility, elasticity, and durability due to the motions frequently experienced by these types of devices. Therefore, the device being too stiff is detrimental to the sensor's productivity [2]. In Figure 1-1 a tactile sensor is determining how to hold a small object, the sensors must be flexible in order for the hand to grasp the ball [5].

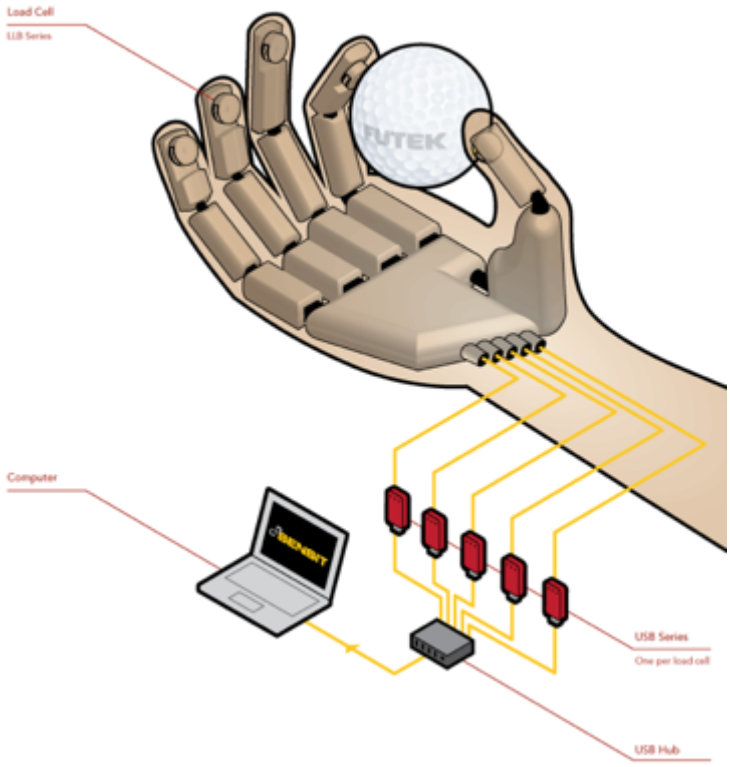

Figure 1-1 Example of a robotic hand tactile sensor-array gripping a small object, the flexibility is necessary for the device to grasp the ball [5].

1.2. Tactile Sensors

Tactile sensors have a variety of applications including pressure and force sensing, dexterous robotics, and surface topography evaluation [6-10]. The fast-

developing world of biocompatible sensing coupled with robotics has led to a need for tactile sensors to be increasingly sensitive, accurate, and most importantly, inexpensively mass-producible. Current technology is limited in the sense that many sensors are made with rigid materials that cannot remain inside or connected to the body for long despite being made of non-toxic materials [6]. As a response, researchers have produced flexible tactile sensors using a variety of methods. Some have been focusing on the biomedical applications of tactile sensors such as artificial skin and biomedical sensing [11] while others can monitor heart rate, body weight measurements, and gastrointestinal health [6].

Artificial skins are designed to be flexible, soft, and elastically deformable [12]. Even in human tactile sensing, children and adults with limited tactile feedback are unable to maintain a steady grip or preform manipulation tasks with their hands [9].The purpose of these skins is to provide a human-like skin membrane to complement the artificial muscles and nervous systems being produced and used by biomimetic robotics.

Just like for humans, dexterous robotics and sensors need tactile data in order to gather information about the world around them. The use of flexible polymers enables the dexterity these tactile sensors find so necessary. These devices often have electrical properties that change when they are deformed. This phenomenon, the changing of electrical properties, can either be caused by the crystallin structure of the material deforming (piezoelectricity) or the friction between particles causing electricity (triboelectricity) [13].

Semi-flexible circuits can be produced utilizing these properties via circuit printing and spray electronics in order to maintain flexibility and elasticity [14]. However, these are not always the most efficient sensors for mass-production. They are

often expensive and fragile. Instead, to achieve this cost-effectiveness, easily scalable sensors are designed using relatively inexpensive materials, reusable molds, and scalable fabrication techniques.

Research groups such as J. Lee et al. [10] and P.J. Sousa et al. [6] have created flexible tactile sensors using polydimethylsiloxane (PDMS) and multiwalled carbon nanotubes (CNTs). For the purpose of this research, sensitivity is determined by the ratio between the device's input signal and the measured output property in question, (voltage, current, temperature, etc). This is discussed more in Section 4.3.

To achieve this scalability, in one case, a skin-like sensors was created using PDMS, nickel powder, and silver nanowires (AuNW) [15]. In this research, the sensing layer is sandwiched between the two non-conducting PDMS layers and the piezoresistive layers are laid down orthogonally. In Figure 1-2, as pressure is applied to the sample, its electrical resistance decreases. Additionally, the flexibility of these sensors is displayed as the sensor is bent over the curve of a computer mouse.

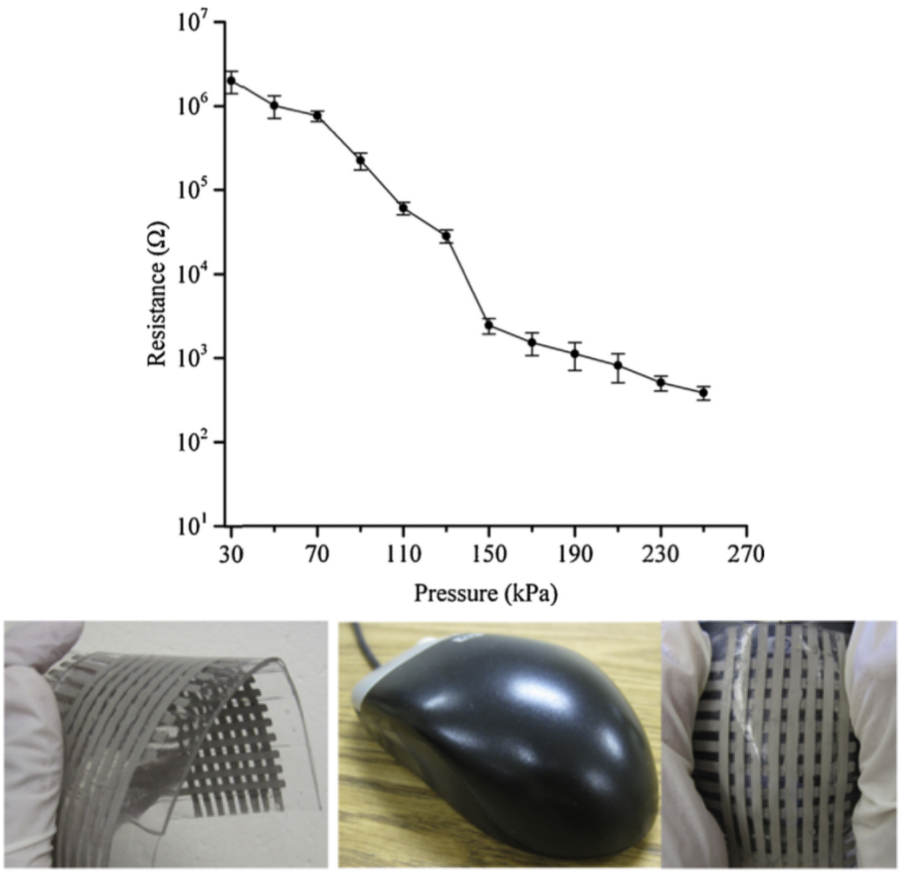

Figure 1-2 Silver/PDMS flexible skin-like sensors (top) response as pressure is applied, (bottom) being flexed around a computer mouse [15].

1.3. Nanocomposites

Nanomaterials and device fabrication can be broken down into two main categories. In the first, nanomaterials are added together in order to produce larger products, a process known as the bottom up approach. Many smaller parts are added together to make a bulk sample or composite. This can be compared to building a sandcastle. The grains of sand are added together to build that castle. The contrary approach is known as top down, where a larger amount of a material is broken down into nano-sized components. This is similar to a wave coming in and eroding away the castle, leaving only a smaller mound behind.

Either way, the nanomaterial must be hosted by a substance that holds the material together. This is done through the use of a matrix. Polymers are a common matrix and can be imbedded with other materials, a process known as functionalization, or adding a filler material to a host in order to change the host material's properties.

An example of a nanocomposite can be seen in Figure 1-3 where the gray matrix serves as a host for the white-colored fillers suspended in it. Different fillers can be used to alter the application of the nanomaterial. For example, metal nanowires or nanopowders (depicted in the figure) are often used to help conduct electricity through otherwise non-conductive matrices. CNTs, especially the metallic CNTs, are a common filler component to create conductive nanocomposites. Other functional materials such as Zinc Oxide (ZnO) and barium titanite ($BaTiO_3$) can also be added into the host polymer to enable piezoelectricity for the nanocomposite.

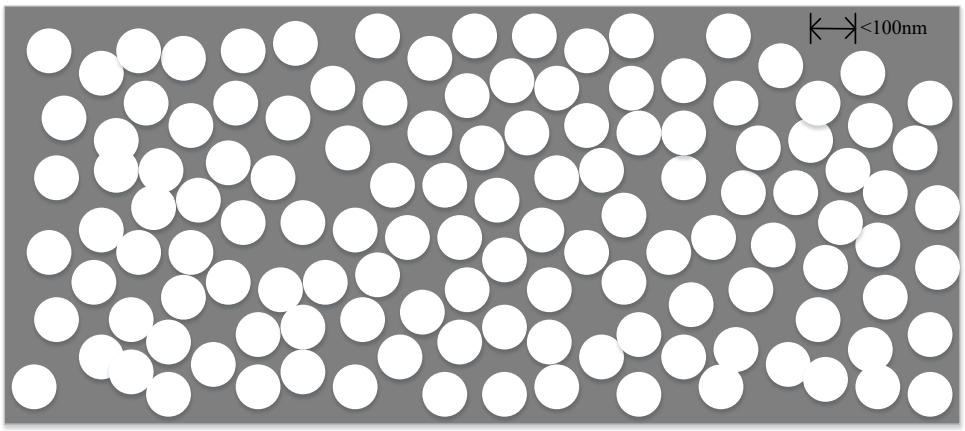

Figure 1-3 A schematic of the nanocomposite material where grey represents the host polymer matrix and white spots are the nanomaterial filler. At least one material must be in the nanoscale in order for a material to be classified as a nanocomposite.

1.3.1. Polymer – PDMS. Polymers are often used as the matrix in nanocomposites because they have a range of baseline electrical, mechanical, and thermal properties. Although the selection of a particular polymer for the nanocomposite depends on the application, most polymers offer similar attractive features such as low cost, high flexibility, and ease of scalability during the manufacturing process. Polymers tend to be more ductile than their ceramic and metallic counterparts, making them advantageous for applications where those stiffer materials would be unsuitable [16]. Furthermore, polymers of different chemical constructs also have different electrical and thermal properties. For example, poly(vinyl alcohol) (PVA) and poly(methyl methacrylate) (PMMA) are both polymers used in graphene based sensors for their electrical conductivity [17], however they have different Young's moduli and electrical conductivities.

A common polymer used in sensor technology is PDMS. PDMS is a thermoset, long-chain polymer renowned for its chemical stability, ease of fabrication, and most notably, its ductility [18]. PDMS is also hydrophobic, an interesting property that makes it usable for filtrations and oil-water separation [19, 20], though that application is not investigated in this paper. The chemical formula for PDMS is $(C_2H_6OSi)_n$ and its chemical structure can be seen in Figure 1-4 [21]. Since it is also biocompatible and relatively inexpensive, PDMS is a promising option for bioimplants and large-scalable sensors.

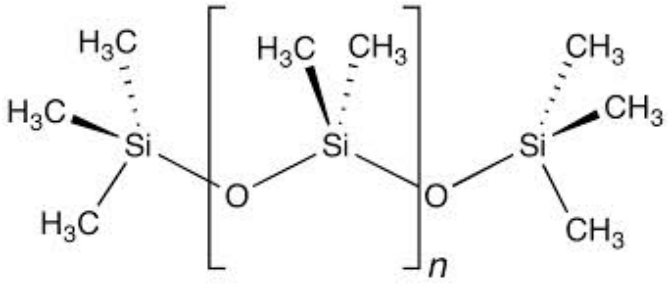

Figure 1-4 Chemical structure for PDMS. Elements present: hydrogen, oxygen, carbon, and silicon [21].

PDMS is so easy to work with because there are so many fabrication techniques that can be utilized to produce functional devices and sensors. PDMS can be spin coated [22], electro-spun [23], screen printed [24], or cast in bulk [25] to create different devices. PDMS can have different mechanical properties for sensitivities at different pressures [26].

Considering all this, PDMS was the chosen polymer for our experiments. A more detailed explanation for the curing parameters and fabrication methods will be covered later in this thesis and are dependent of the applications of the devices. However, as PDMS is insulating, a conductive filler must be added to enable the conductivity of the final composite. This technique is called the conductive polymer approach and is often used for these types of applications [11].

Several suitable fillers have been identified by various papers. These include, but certainly are not limited to, nickel, nickel-copper alloys, and CNTs [6, 27-30]. PDMS-CNT based tactile sensors are suitable for both biomedical and tactile sensing applications [31, 32]. In the cases where conductivity is required, a conductive filler must be added into the host polymer in order to generate a functional nanocomposite [33, 34].

1.3.2. Carbon nanotubes.CNTs were first discovered in 1991 and have since been explored for their impressive electrical, mechanical, and thermal properties. Sensors made from CNTs have a vast scope of applications including biosensors, drug delivery, nanowires, superconductors, and many others [35]. CNTs can be stretched to nearly five times their original length completely plastically [36]. This is so important because it means that CNTs can be used a structural reinforcement inside other matrices. This is caused by the shape of CNTs, which is essentially just a sheet of graphene rolled up into a single-layered, nano-scaled rod.

A single-layer CNT is known as a single-walled carbon nanotube (SW-CNT). If there are two concentric layers in the structure, the CNT is known as a double-walled carbon nanotube. Finally, the most common type of carbon nanotube is one with several layers of graphene, known as a multiwalled CNTs (MW-CNT) [37]. An example of each can be seen in Figure 1-5 [35]. This tubular type of structure means that the outer layers of the nanotube are strong and durable, while maintaining a hollow (and therefore light-weight) core [38]. They can also be doped with other metals for functionalization, but more commonly, they are mixed into a matrix as part of a nanocomposite.

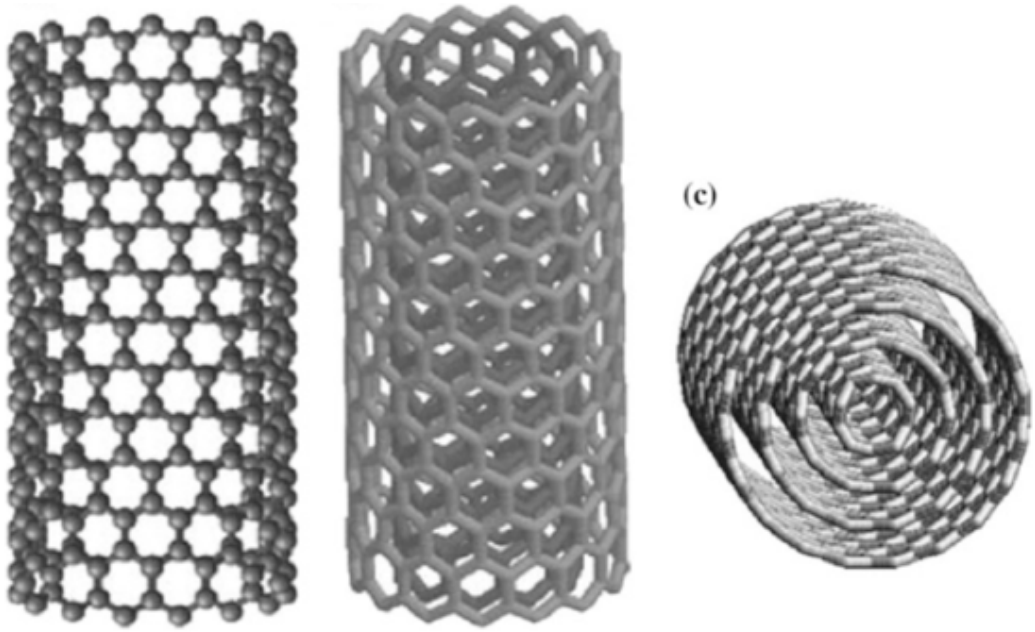

Figure 1-5 Various types of CNTs: single-walled CNT (left), double-walled CNT (middle), and multiwalled CNT (right) [35].

CNTs also have a chirality, and their electrical properties depend on the direction or "handedness" of the enantiomers [1, 39, 40]. Depending on the orientation, the CNTs can be either metallic or semiconducting. About 66% of all CNTs are semiconducting, while only 33% are metallic. This is caused by the differing band gaps in the two enantiomers. Different orientations of the carbon atoms can cause the CNT to have a "zigzag" structure, an "armchair" structure, or a generic "chiral" structure, as illustrated in Figure 1-6 [41]. A weigh boat filled with 95% pure multi-wall CNTs is pictured in Figure 1-7.

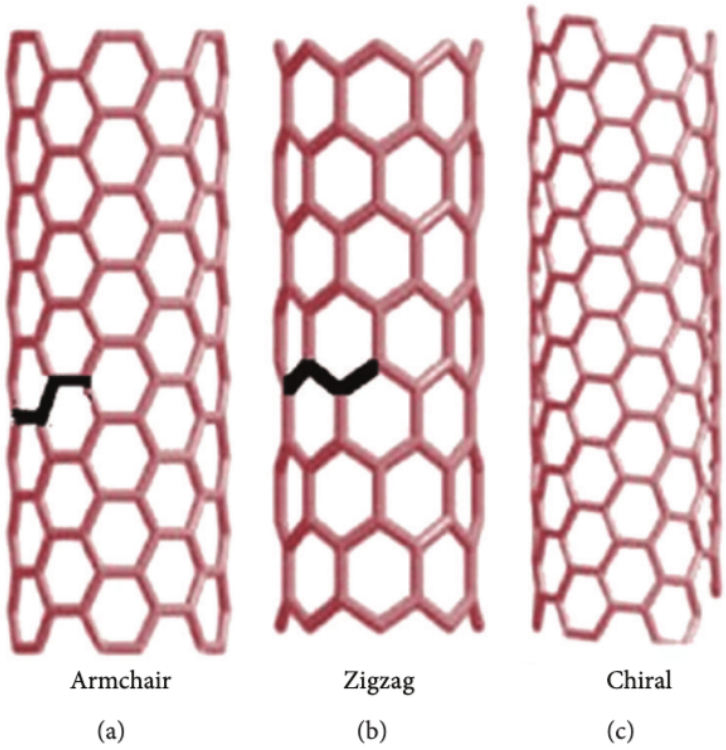

Figure 1-6 Chirality in CNTs: (a) armchair shape, (b) zigzag shape, and (c) chiral shape [41].

Figure 1-7 MW-CNTs in weigh boat, 95% purity, 10-20 nm dia. 10-30 μm length.

Furthermore, CNTs are piezoresistive [42], meaning that their resistance changes as the material is deformed. This allows the sensors to have a measurable sensitivity which detects not only if there is pressure being applied, but also how much pressure is being applied. Combined with their extreme plasticity, CNTs are a great candidate for sensors that will be repeatedly deformed.

Because nanomaterials, especially CNTs, are small and tend to get tangled among themselves, CNTs often need to be dispersed using an agent. This can eliminate agglomerations as the material is added to the matrix [43]. The processes that can be used for dispersion are discussed more thoroughly in later chapters.

1.3.3. Zinc oxide. Another filler that is often added to PDMS is ZnO. ZnO comes in various shapes and sizes including nanorods of various lengths and nanoparticles of various sizes [44]. ZnO is a popular choice for researchers for its bio-safe and antibacterial properties [45]. Furthermore, it has piezoelectric properties, meaning that it produces electricity when deformed. ZnO can be added to different materials in various concentrations in order to increase the piezoelectric output [46].

ZnO nanowires or nanoparticles can be used for actuators, sensors, and energy harvesting devices. This can be achieved through different fabrication methods including spin coating to generate thin films and casting to produce larger bulk samples [47]. ZnO can be purchased from VWR as nanoparticles with varying sizes, ranging from 20 nm to 200 nm. For the purpose of this research, 20nm, 99.5% purity ZnO was purchased and used in experiments. An image of the ZnO nanoparticles used in these experiments can be seen in Figure 1-8.

Figure 1-8 ZnO, 29 nm, 99.5% purity in weigh boat.

1.4. Forming Nanocomposites

In order to avoid agglomerations and uneven distribution of CNTs in the PDMS, CNTs need to be suspended in a dispersion agent or dissolved into a solvent prior to mixing with PDMS. Several agents are studied with varying degrees of success. Some are very suitable to suspend CNTs while others are less so. Examples of dispersion agents that have been studied are toluene, tetrahydrofuran (THF), chloroform, and dimethylformamide (DMF) [48].

While DMF had the best dispersion for CNTs, it caused a reaction with PDMS, making it unsuitable for a CNT dispersion in PDMS. Toluene was found to have the best dispersion for the PDMS but had poor solubility of CNTs. This makes it also unsuitable for dispersion [48]. Ultimately, it was discovered that the chloroform suspended the CNTs in a stable solution that mixed well without augmenting the PDMS. Other possible agents were isopropyl alcohol (IPA) and ethanol.

1.5. Porous Nanocomposites

Porous structures are found throughout nature and living organisms and serve a variety of purposes [20]. Scientists and researchers often look to nature for inspiration and optimization. This influence has led to interesting adaptations of some of nature's most efficient porous solutions. Progress in stretchable, porous, and/or biocompatible materials has led to an increasing interest in their applications for nanocomposites. More specifically, tactile sensors, energy harvesters, and other piezoresistive/piezoelectric nanocomposite-based devices have been created using biologically inert materials [20, 42, 49]. Devices with porous structures have been gaining interest for their decreased cost, improved deformability, and comparable sensitivity. These porous nanocomposites have applications in biomimetics, filtration, tactile sensing, and energy harvesting [19].

These porous structures could be used in functionalized materials, creating nanocomposites. The purpose of foaming the sample is to allow for greater deflection in the sample during compression. This will hopefully lead to more sensitive samples that can detect pressures at a finer resolution than those of solid or thin-film samples [26, 50, 51]. Additionally, foam samples require less materials than bulk samples, effectively reducing the cost of raw materials during fabrication. These porous devices have reliable performance despite repetitive loading and unloading of the samples, making them prime candidates for robotic applications [52].

In addition to adding different nanomaterials to PDMS and altering its curing parameters, another way to tune its mechanical properties is through the use of adding and altering a porous structure. By controlling the density of the pores in PDMS, the Young's modulus can be changed. The modified materials can be stiffer or more ductile

according to their applications. Porous samples are more flexible and deform easier, making them more suitable for ergonomics than solid PDMS.

Pores can be formed using a variety of techniques with each producing a different type of structure. Most structures can be broken down into two categories, opened pore structures or closed pore structures [20]. Open pore structures have interconnected pores inside the material. Gasses and liquids are permitted to permeate the entire structure through these interconnections, known as throats. An example of an open pore structure is a kitchen sponge. Materials with this open structure are generally softer and more deformable than their closed pore counterparts.

Closed pore structures, on the other hand, have pores that do not interconnect. Instead, the gas or liquid that is filling those pores is trapped in the cells. This leads to stiffer materials that do not deform as much. An example of such a material is PVC piping, which has a closed pore structure. The result of this type of structure is a light-weight but rigid material.

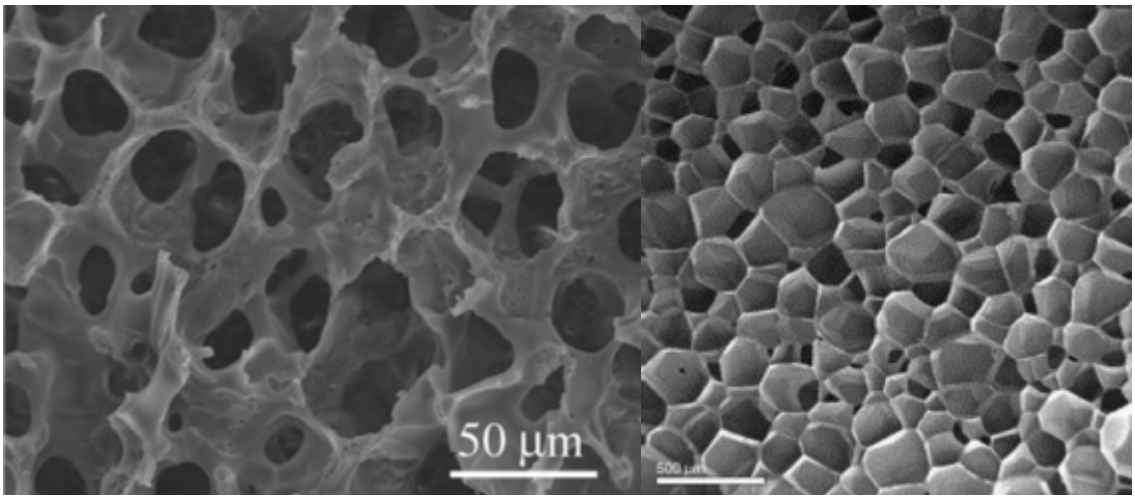

Figure 1-9 Open pore structure (left), more flexible with interconnected pores with throats between cells [53]; closed pore structure (right), no connection between pores, more rigid then open pores [54].

Depending on what kind of material properties are desired, either structure can be used. Chemical blowing is often done to produce closed pores, but the pore size is often hard to predict and rarely consistent [55, 56]. Chemical blowing is process in which a blowing agent produces a cellular structure, usually with the aid of a chemical reaction or increased temperature. The material hardens, sometimes condensing, and causes the material to constrict again [57]. Bubble nucleation, or cell formation is often controlled by the viscosity and thickness of the thermoplastic material [58]. When the material sets, the re-condensing chemical blowing agent does not shrink the pores. However, the inevitable inconsistency is undesirable since unpredictable stress concentrations result from unpredictable pore structures.

Instead, to produce interconnected pores of a consistent, predicable size leeching or scaffolding is a common method [20, 59]. In this process, a sacrificial scaffold material is mixed into the nanocomposite and removed later on. For its non-toxicity, cost-effectiveness, and predictable particle size, sugar was the sacrificial ingredient for many

experiments [19, 52, 53]. In order to vary the pore size, different types of sugar were used. Brown sugar (largest pore size), granulated sugar, and ultrafine sugar (smallest pore size) were mixed into the nanocomposite and dissolved out after curing. This process is detailed in section 2.3 as a part of the fabrication process.

Piezoelectricity and piezoresistivity are both explored in this paper, so understanding the difference is paramount. Piezoresistivity is where the compression of a material causes nanofillers (such as CNTs) to connect and therefore reduces the resistance of the material during compression. Piezoelectricity, on the other hand, is a voltage generated by a piezoelectric material such ZnO when the material is deformed. Figure 1-10 shows the difference between the piezoelectric and piezoresistive effects to make things clearer.

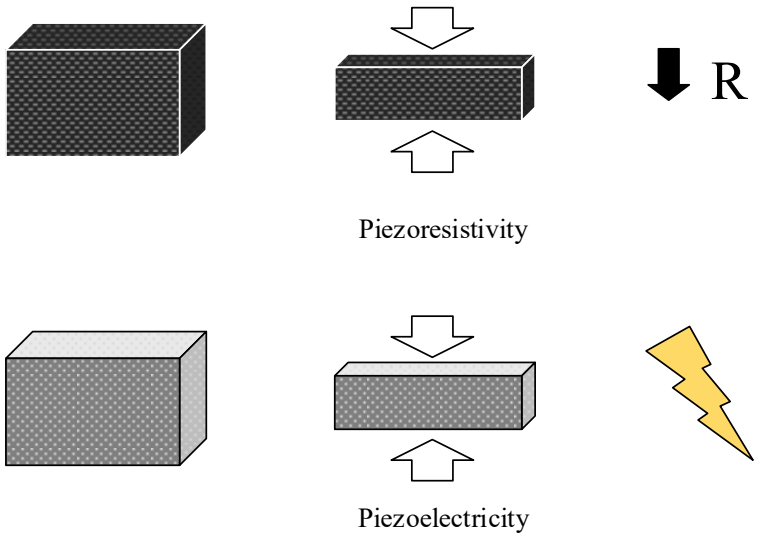

Figure 1-10 Piezoresistivity vs. piezoelectricity. Piezoresistive material is deformed and the resistance is decreased, piezoelectric device is deformed, and a voltage is created.

1.6. Piezoresistivity.

Piezoresistivity is a phenomenon where the electrical resistance of a material changes depending on how much pressure is being applied to the device [31]. CNTs are often chosen as a piezoresistive material because they are easy to work with and relatively inexpensive. Devices made from CNTs and PDMS are often chosen for tactile and pressure sensing since the change in resistance is predictable [31, 60].

In order to gather data over a larger area, it is often helpful to arrange several sensors in arrays or matrices. This was done in one instance where researchers were gathering information about water pressure and marine movements [60]. Many of the large-scale piezoresistive sensors that have been developed sacrifice location accuracy in favor of larger area sensors. For example, Adafruit sells a piezoresistive sheet 11” by 11” that can detect when pressure is applied anywhere on the sheet but not precisely where [61]. More developed technologies are being created labs but are not yet commercially available due to scalability issues[62]. Regardless, several types of piezoresistive sensors have predicable changes, which is what makes them so applicable for sensors.

The combination of CNTs and PDMS do not generate any electricity. For this, a piezoelectric material must be used. ZnO is often added a matrix to harness its piezoelectric properties [63, 64].

1.7. Piezoelectricity.

The growing interest for alternative portable power has forced interest towards piezoelectric energy harvesters. Such devices can generate electricity based on the ambient movements around them; using the right materials, the applications are enormous. This variety has made piezoelectric energy harvesters and sensors an

appealing option for researchers [65]. For example, piezoelectric sensors are capable of wirelessly transmitting data about structural health in bridges and other large-scale civil projects [66].

On a smaller scale, piezoelectric devices made from biologically inert materials can be implanted in the body and used to power many different apparatus [67]. Many current bio-implantable devices have batteries that need to be changed every few years [67], Since battery replacement means surgery for people with implant, this is a distasteful option due to the risks associated with surgery. Piezoelectric harvesters, however, avoid this unnecessary risk because they generate electricity for themselves as opposed to relying on an external charge, eliminating the need for surgeries to replace batteries.

In such cases, the bio-implantable device must be made of biologically inert materials. ZnO is a known piezoelectric material, meaning it is capable of generating electricity when deformed. It can be used as an energy harvesting device or as a piezoelectric sensor when embedded into a PDMS-CNT nanocomposite. Devices using ZnO and CNTs were capable of achieving up to 7.5 V output during testing [63]. Furthermore, ZnO can also be used in biosensing application, is was done in Georgetown University [44]

When a device produces electrical response through piezoelectricity, it does so along its dipole. In order to maximize the voltage output of piezoelectric devices, these dipoles can be aligned. This forces all of the electrical outputs of the particles in one direction, a process known as poling [47, 68, 69]. Samples that have undergone the

poling process have proven to produce more electrical output than those that have not, meaning it was a natural first step for researchers to study [47, 67].

Dipole alignment is achieved when an electrical field is forced through a piezoelectric device. This forces all the dipoles of the piezoelectric material, in this case ZnO, to align in the same direction, as shown in Figure 1-11. With the aid of heat and a long poling period, eventually the dipoles of the sample will align.

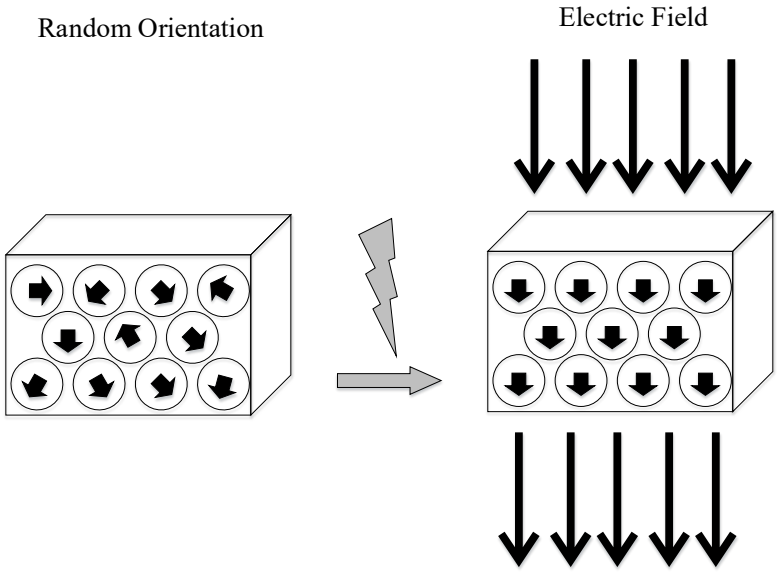

Figure 1-11 Dipole alignment occurs under a strong electric field. Piezoelectric materials produce voltage (in the direction on the arrows) when deformed. Randomly arranged particles subject to a high voltage and temperature re-align themselves to generate this electricity in a uniform direction when deformed after dipole alignment.

Dipole alignment can be achieved using two parallel capacitor plates placed near each other. One plate is supplied with an electrical voltage and the other connected to ground, creating a potential between the two plates. The strength of this field is determined by the equation:

$$E = \frac{V}{d} \quad [1]$$

where E is the electric field strength, V is the voltage supplied (V), and d is the distance (m) between the two plates. Several research groups use this process to improve the output voltage of their samples. The parameters that they used to pole their devices are marked in Table 1-1.

Table 1-1 Proposed dipole alignment parameters

Author	Poling Voltage (kV)	Temp. (C)	Time (hrs.)	Cited Initial Output (ppV)	Cited Poled Voltage (ppV)	Initial Current Output (pp) (mA)	Poled Current (pp) (nA)	
Park, et al. [70]	0.5	140	12	0.3	14	-	-	
	1	140	12	0.3	16	-	-	
	2	140	12	0.3	20	-	-	
Park, et al. [22]	~1.5	150	20	0.4	5	12	100	100kV/cm
Jeong et. al. [71]	0.5	150	-	<1	5	<1	7000	
	1	150	-	<1	7	<1	8000	
	2	150	-	<1	12	<1	1200	
Yang et al. [13]	0.675	20	12	-	6	-	-	4.5 kV/cm

1.8. Objectives

In this research the effects of porosity, pore structure, and nanocomposite concentrations are studied to determine an optimal configuration for sensing applications. Our research has explored the effects of adding various nanoparticles to PDMS and quantified the performance of the resulting nanocomposites. These devices have been successfully used as pressure sensors and energy harvesters. Porous structure variation for piezoresistive and piezoelectric materials is studied. Here, varying the porosity, pore

shape, and the density of CNTs is explored for use in pressure sensing and energy harvesting. While devices have been fabricated using sugar scaffolds, currently the investigation of porous structures on piezoresistive/electric devices is limited and largely unprecedented. The goal is to begin a study on these variations. The mechanical and electric properties of several foamed structures are tested in order to assess their performance as sensors.

The objectives of this research include;

1) Create a well-dispersed nanomaterial with PDMS, CNTs, and ZnO.
2) Test mechanical properties of various porous structure. Determine which structure has most consistent mechanical properties.
3) Produce pressure sensing CNT-PDMS-based porous nanocomposites devices.
4) Develop piezoelectric energy harvesters using ZnO in nanocomposite.

1.9. General Layout of Thesis

In Chapter 2 of this thesis, various fabrication techniques are explored. The quality of two techniques are compared to each other using scanning electron microscopy (SEM) inspection. Using the methods developed here, samples were fabricated for an investigation of the effects of different porous structures including various scaffolds (three different sugars, citric acid, and sodium bicarbonate) at various densities in Chapter 3. In Chapter 4, these devices are functionalized using CNTs to produce pressure sensors. Piezoresistive pressure sensors were fabricated using different concentrations of CNTs. Further, devices were fabricated using different porosities. In Chapter 5, a combination of CNTs and ZnO nanofillers used to fabricate piezoelectric energy harvesting devices. Both thin-film and bulk samples are fabricated. Several sugar

scaffolds are explored and the effects of these scaffolds on the devices' mechanical properties are tested. Devices undergo dipole alignment in order to amplify their electrical output. Finally, the paper is concluded, and future works are discussed in Chapter 6.

Chapter 2

Fabrication of Nanocomposites

2.1. Foamed Nanocomposites

Wearable electronics, tactile sensors, and energy harvesters have seen great improvements as "foamed" or porous structures [9, 51, 63]. Foamed structures are believed to produce more flexible samples while also cutting costs on materials. In this chapter, various ways to foam or make pores in PDMS are explored including chemical blowing and scaffolding. Both methods provide their own benefits and shortcomings but scaffolding clearly presents itself as a more suitable method for the proposed applications.

Samples were studied both as tactile sensors and as energy harvesters by adding fillers to the PDMS. This effectively changes the function and therefore application of the porous nanocomposite. As described above, CNTs have a piezoresistive property that makes them great candidates for tactile pressure sensors. Additionally, ZnO, a piezoelectric material, generates a voltage when the samples are deformed. Provided the earlier stated biocompatibility and polar structure, ZnO is a prime candidate for nanocomposites for piezoelectric energy harvesters and sensors.

At the University of Adelaide (Australia) one research team used store-bought sugar cubes as a leeching scaffold for non-functionalized PDMS. In this study, the oleophilic/hydrophobic PDMS can actually adsorb oil from water in an oil spill [19]. Another group uses a dissolvable sugar scaffold to aid in formation of a nanofibrous tissue using PLLA [53]. Many other studies are conducting using this direct templating technique [20]. These studies serve as the basis for our sugar scaffolding. Using similar techniques to what was described in these papers, various types of sugar were studied at

various densities in order to adjust the mechanical properties of the functionalized PDMS devices.

For this study, porous nanocomposite sensors and energy harvesters are studied to understand the effect of porosity on the sensors' functionality. Samples were mechanically deformed to assess their moduli of elasticity and their electrical properties under loading. Further, samples were inspected using scanning electron microscopy (SEM) to ensure good dispersion of nanocomposites throughout the PDMS matrix.

2.2. Distribution of Nanomaterials

In this section, two dispersion agents were studied along with a control group of samples made without a dispersion agent. Three types of samples were fabricated in total. Isopropyl alcohol (IPA) and chloroform were studied as two possible solvents for the CNTs based on what was reported in [48]. Hand mixing nanocomposites directly into the polymer was also studied as a slightly different process. In the section below, the methods are described for each, detailing how the CNTs were mixed into the PDMS and the results of the dispersion are shown using SEM inspection.

Materials were purchased from vendors; the specifications of those materials can be seen in Table 2-1. The amount of each material is not mentioned in this section because depending on the test being conducted, different amounts were used. Instead, these recipes can be found in their respective chapters.

Table 2-1 Material specifications for devices in this thesis

Material	Purity	Dimension	Vendor
MW-CNTs	95%	10-20 nm dia 10-30 μm	Nanostructured and Amorphous Materials
ZnO	99.5%	20 nm	Nanostructured and Amorphous Materials
PDMS	N/A	N/A	Dow Corning
Chloroform	99.99%	N/A	VWR
Isopropyl Alcohol	99.9%	N/A	VWR
Ultrafine Sugar	Food grade	N/A	Store bought
Granulated Sugar	Food grade	N/A	Store bought
Brown Sugar	Food grade	N/A	Store bought
Citric Acid	N/A	N/A	Thomas Scientific
Sodium Bicarbonate	N/A	N/A	Thomas Scientific

2.2.1. Mechanical Mixing. For this set of experiments, a somewhat homogeneous nanocomposite was fabricated by mechanical mixing. While this was ultimately determined to be not as uniform as originally believed, many papers describe mixing by hand with a spatula or mixing with a magnetic stir bar as suitable methods for preparing devices, so it is used as a baseline for fabrication techniques [32, 72, 73].

In order to ensure the samples had minimal agglomerates, materials are added in a specific order, at a gradual pace. If the material is being made into a piezoelectric device, first, ZnO and CNTs are weighed and mixed until all visible clumps and aggregates were gone. This is done with a metal spatula and takes around 5-10 minutes depending on the humidity and static electricity levels in the room. These materials can be seen in Figure 2-1. If the sample is to be piezoresistive, only CNTs are weighed out and the portions where ZnO is mentioned in the instructions can be ignored.

The proper amount of scaffolding material, or leaching agent, is measured out but not added to the ZnO-CNTs mixture. Instead it is kept off to the side. The PDMS and the curing agent are weighed out at a 10:1 ratio, and the curing agent is poured into the

PDMS. The two are stirred by hand for at least three minutes. The ZnO and CNTs mixture is gradually added to the room temperature PDMS-curing agent mixture, until the entire sample is mixed completely (~5 minutes). Since samples are designed to be porous, de-bubbling of the mixture in a vacuum chamber is not necessary for this process. Figure 2-2 depicts the process for making hand-mixed samples.

Figure 2-1 ZnO and CNT nanopowders before (left) and after mixing (middle); PDMS before de-bubbling (right).

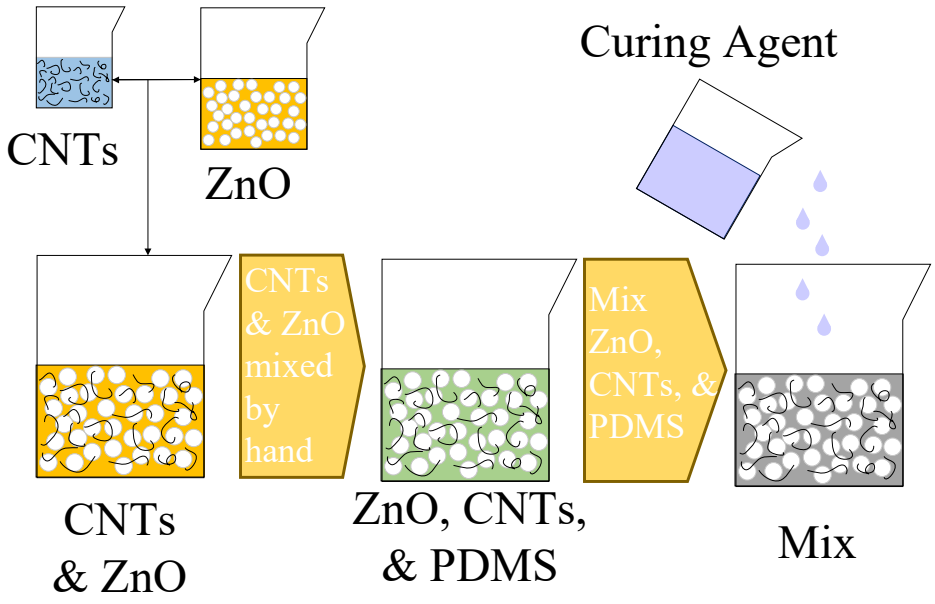

Figure 2-2 Process flow for hand mixing piezoelectric devices. CNTs and ZnO are weighed and mixed together. CNT-ZnO is added to PDMS, mixed well, then curing agent is mixed in.

2.2.2. Dispersion method. Because mechanical mixing is not the most reliable method for avoiding agglomerations, a dispersion method was tested as well. In this method, two different dispersion agents were explored, and one was decided upon. A schematic of how the devices are fabricated can be seen in Figure 2-3.

During these experiments, many of the steps are similar to what is described earlier for mechanical mixing with a few key differences. Firstly, the CNTs and the ZnO are kept separate after they are weighed out instead of being mixed together. CNTs are added to a watertight tube with the dispersion agent (either isopropyl alcohol or chloroform) and sonicated in a tub for 30 minutes. Then, PDMS is weighed into a petri dish (without the curing agent) and placed on a hot plate with a stir bar set to 120°C. The stir bar is not turned on yet. This heats up the PDMS to make it less viscous and easier to mix. Once the PDMS is warmed up, the stir bar can be set to a speed of 60 rpm.

Next, when the CNTs have been completely suspended, the CNT/solvent is added to the PDMS. It is important to avoid splashing, lest the actual CNTs concentration will be less than what is measured out. The dispersion agent may need to be boiled out in bursts before more CNTs/dispersion agent can be added if the petri dish gets full before all of the CNTs are added to the dish. Add the ZnO to the petri dish next while there is still dispersion agent in the dish to ensure the ZnO achieves a good dispersion into the PDMS. Figure 2-4 shows the CNTs in the chloroform with the PDMS in the petri dish. The mixture is then continuously stirred until all of the solvent has been evaporated. This results in leaving a well-mixed composite of PDMS, CNTs, and ZnO. The mixture must be brought down to room temperature after all the dispersion agent has evaporated. Finally, the curing agent can be added to the sample and stirred for at least five minutes to ensure a uniform mixture.

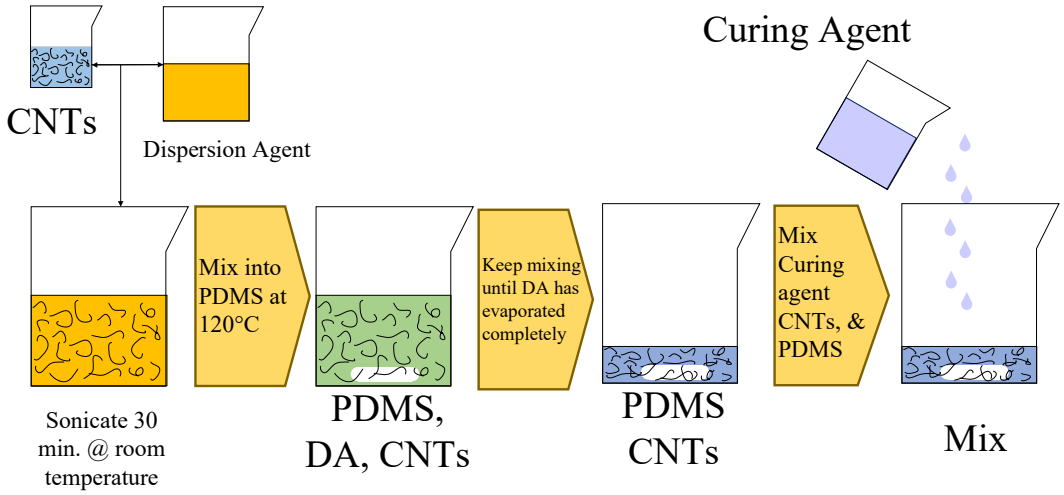

Figure 2-3 Dispersion method for mixing nanocomposites. CNTs are added to dispersion agent (DA) and sonicated at room temperature for 30 min. Suspension is mixed into PDMS on a hot plate (120°C) and stirred at ~60 rpm. If applicable, ZnO is added to the mixture. Dispersion agent eventually will evaporate completely, and composite is allowed to cool to room temperature. Curing agent can then be added and mixed well into the mixture.

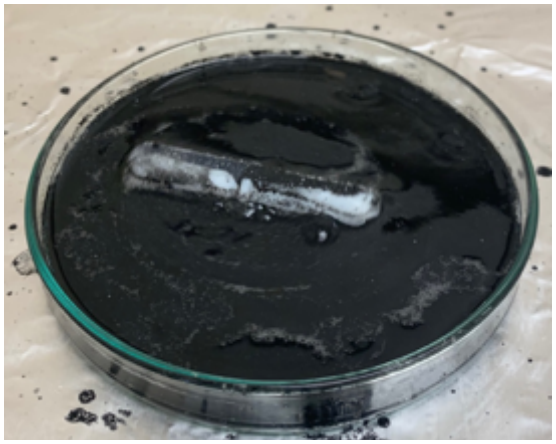

Figure 2-4 CNTs in chloroform being mixed with PDMS on hot plate. Chloroform is evaporating out of the PDMS/CNT composite.

2.2.3. Dispersion agents. In this set of experiments, two different dispersion agents were used based on previous reports [6, 24]. Isopropyl alcohol (other names: IPA, rubbing alcohol, isopropanol) and chloroform, an organic solvent, were studied [49]. There is no exact amount of dispersion agent that needs to be used, however, enough should be used to completely submerge the CNTs with ample extra dispersion agent. After sonication, there should be no agglomerations of the CNTs in the dispersion agent. If there are, more dispersion agent is needed.

IPA was tested first because it is inexpensive and was readily available in the lab. It proved to suspend the CNTs well and not react with the PDMS negatively. However, CNTs did not remain suspended for long: separation was apparent after about an hour but the mixture could still be used; however, after a week, the separation of the CNTs from the dispersion was so severe that re-sonication would be necessary (Figure 2-5).

Alternatively, chloroform suspended the CNTs well and also did not react with the PDMS. Additionally, the solution is more stable, with a shelf life of over 1 week with adequate suspension of CNTs. A drawback, however, was that in order to use chloroform, experiments must be carried out under a fume hood with extreme care. While this is not a terribly uncommon or cumbersome task, it did require that all the materials be move to and from the lab with a fume hood in order to conduct experiments.

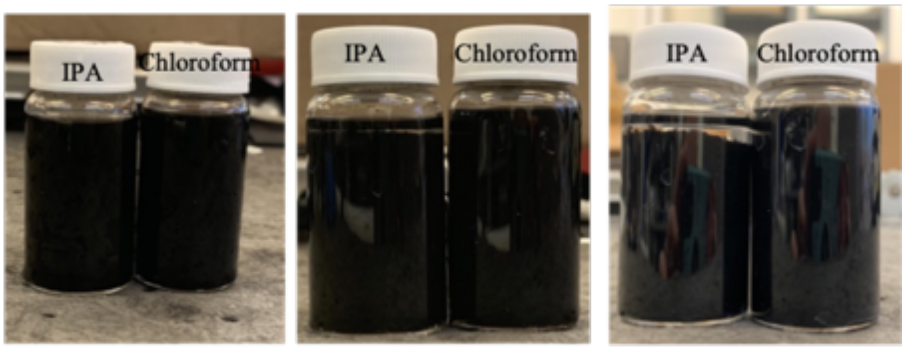

Figure 2-5 Stability of CNTs in IPA and chloroform. Right after sonication, both agents appear to have successfully suspended the CNTs. After 1 hour, separation becomes apparent, and by one week after sonication, suspension has settled.

2.3. Sample Fabrication – Sugar Scaffolding

In order to fabricate porous devices, the scaffolding material is added to the composite after the curing agent is added but before the samples cured. PDMS needs both the curing agent and heat to cure fully, so as long as the composite is kept at room temperature, there is sufficient for the scaffolding agent to be added into the PDMS/curing agent mixture. The scaffolding material must be mixed entirely into the PDMS. As pouring it all at once leads to non-homogeneous samples, the scaffolding agent is added to PDMS in small bursts to ensure the homogeneity. This is especially important for samples with higher pore densities where the amount of scaffolding material is significantly higher than the PDMS nanocomposite. The entire mixture is poured into molds of an appropriate size, as depicted in Figure 2-6. Depending on the tests, molds were either 1” × ¼” × ¼”, or ½” × ½” × ¼”. Finally, the sample is cured on a hot plate at 90°C for four hours.

Three types of sugar including ultrafine sugar, granulated sugar, and brown sugar were studied. Several different pore densities were studied in order to gain insight into

the mechanical properties of the porous samples. Samples were made with as low as 40% scaffolding agent, however samples made with less than 60% scaffolding agent showed clear settlement of the scaffolding material, making visible layers in the samples. For this reason, only 60%, 70%, and 80% sugar scaffolds were tested for this project.

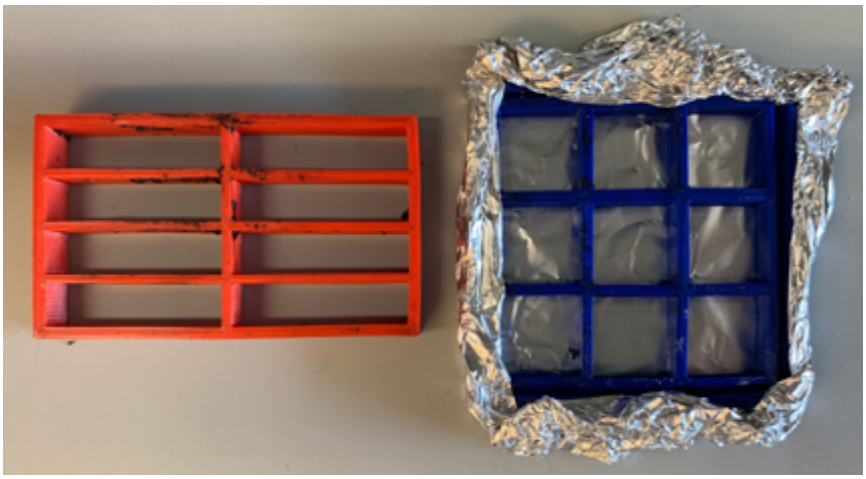

Figure 2-6 Molds used for sample fabrication (left, mold for tensile tests, 1” × ¼” ×¼”: right, mold for electrical resistance testing, ½” × ½” × ¼”.

Once the sample was fully cured, the scaffolding material must be removed from the host matrix for these test-sized samples. In the case of sugar scaffolds, a boiling or warm water bath was used to dissolve the sugar. Figure 2-7 is a visual representation of how the sugar is removed from the host matrix, turning a solid sample into a foamed structure.

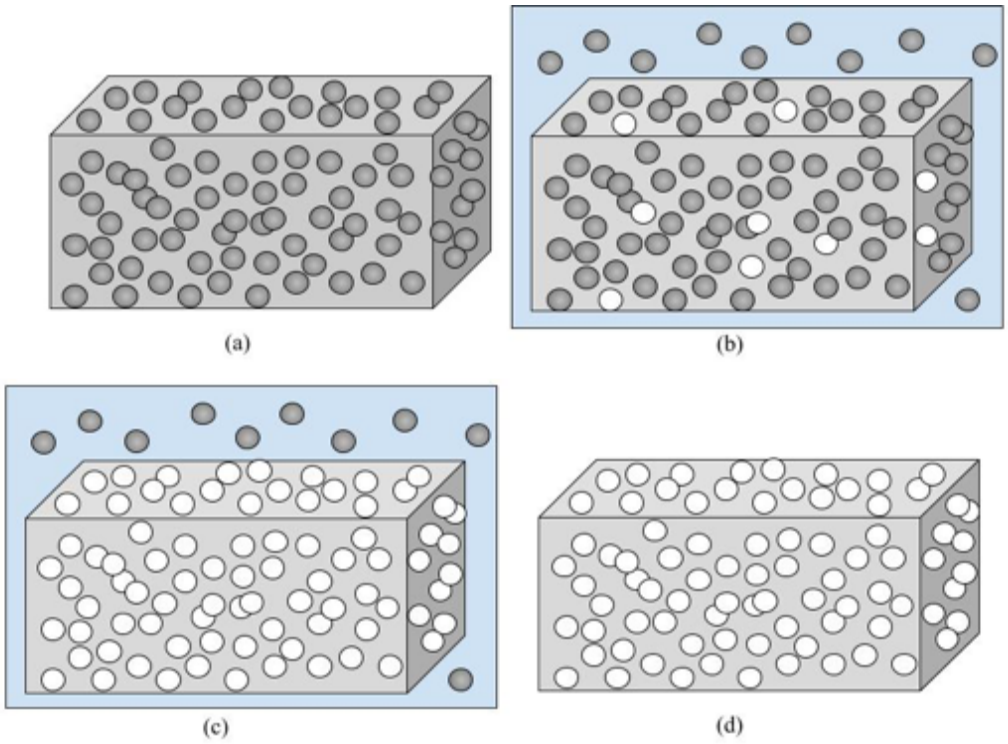

Figure 2-7 Scaffolding process for producing porous structures. (a) Sample with sugar embedded. (b) Warm water begins to remove sugar. (c) After several hours, sugar is dissolved from sample. (d) Sample is removed from water, leaving foamed PDMS nanocomposite.

After all the sugar was removed and samples were thoroughly dried (could take 12-48 hours), various tests could be done on the samples. Samples were evaluated using SEM, tensile testing, and electrical output testing. Each of these tests provides useful information on the functionalized materials, the porous structures, or the resulting piezoelectric or piezoresistive devices. Samples made from these methods had consistent structures, densities, and good distribution of nanomaterials.

2.4. Sample Fabrication – Thermal Decomposition

To complete a thorough investigation of porous structures, a set of experiments was conducted centering around different materials that could form pores. Anhydrous

citric acid and sodium bicarbonate were studied as two possible foaming agents instead of sugar [38, 51, 71, 74]. These materials replaced the sugar in the fabrication process.

An interesting difference between the sugar and these other materials was that neither citric acid nor sodium bicarbonate was dissolved in water like the sugar samples. Instead, citric acid was thermally decomposed on a hot plate in a fume hood at 150°C. This was done overnight until a soft foam was left behind. Sometimes rinsing the sponge afterwards and allowing it to dry could wash off any residue from the citric acid. Figure 2-8 is a visual representation of how the citric acid is thermally decomposed from the PDMS matrix. Sodium bicarbonate was dissolved in acidic acid at room temperature, overnight in most cases. This is done similarly to the way that sugar was removed, just with acidic acid instead of water. To speed things along, a magnetic stir bar could be placed in the beaker to keep fresh acidic acid moving across the sample's surface. As with the citric acid samples, these too were rinsed in water to remove any residual reactant on the sponge.

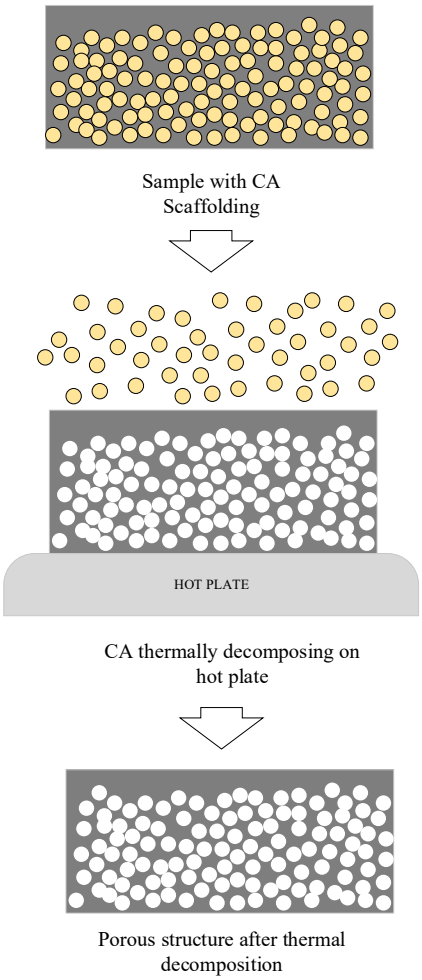

Figure 2-8 Thermal decomposition of citric acid to create foamed samples. Sample made with anhydrous citric acid is placed on a hot plate at 150°C thermally decomposes. It expands into a gas, if the gas gets trapped it forms a closed pore structure, or an open structure if gas is able to escape. The result is a foam sample.

Similar to the sugar scaffold, samples made with insufficient sodium bicarbonate or citric acid experienced separation, (see Figure 2-9). However, unlike the sugar, these materials showed separation at different pore densities. Citric acid showed separation at 60%, but not 70%, while sodium bicarbonate showed separation at all levels except the highest, 80%. This is likely caused by the differing densities of these materials producing separation as the PDMS is curing.

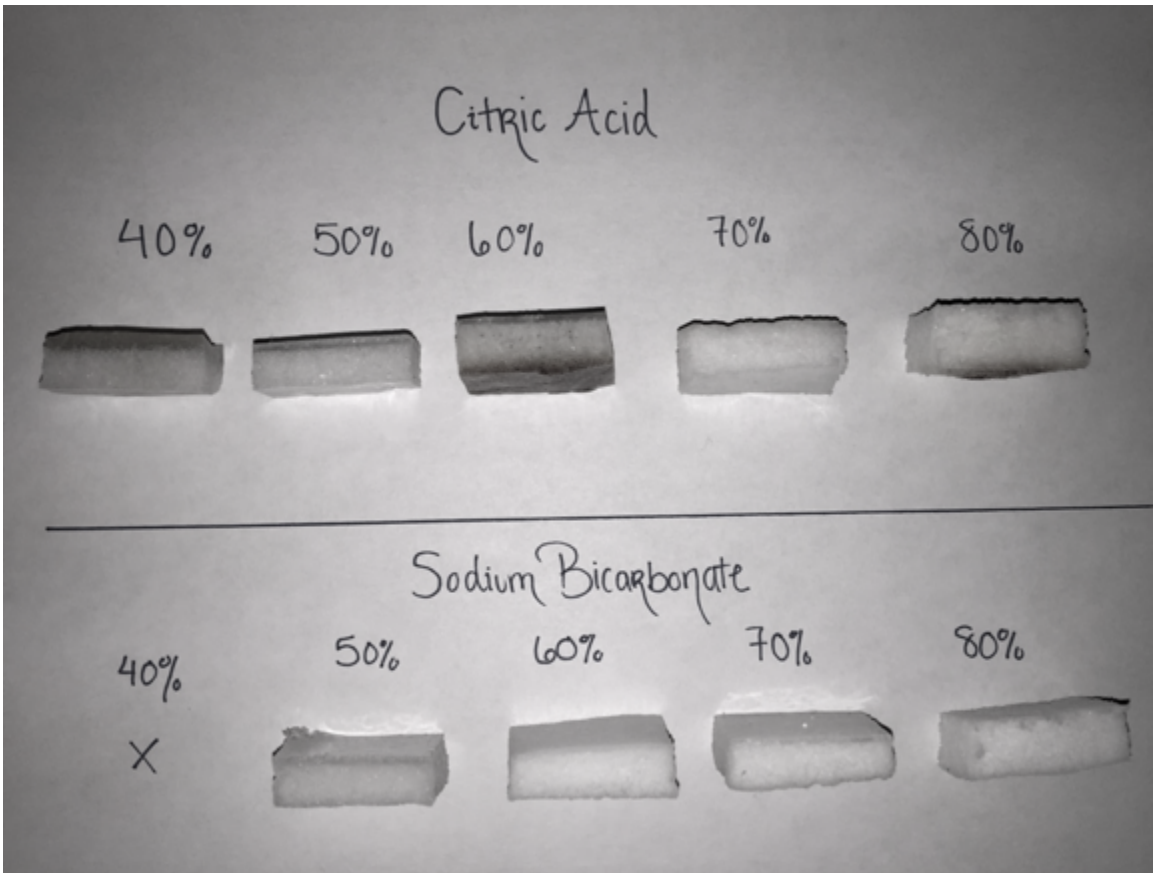

Figure 2-9 Citric acid and sodium bicarbonate-based foam samples without functionalization. Citric acid samples could be burned during decomposition, both scaffolds experiences separation at all but the highest pore concentrations.

2.5. SEM Inspection

In order to determine the effectiveness of the dispersion agents, SEM images were taken of samples made with both mechanical mixing and dispersion methods. In Figure 2-10, a sample made with mechanical mixing is shown. ZnO from the mechanical mixing method is clearly not dispersed uniformly throughout the sample. These are shown as white spots on the host matrix. This figure shows that the hand mixing method does not disperse the ZnO or the CNTS well in the matrix. It is worth noting that the ridges were likely caused by the cutting tool when the sample was being prepared for imaging.

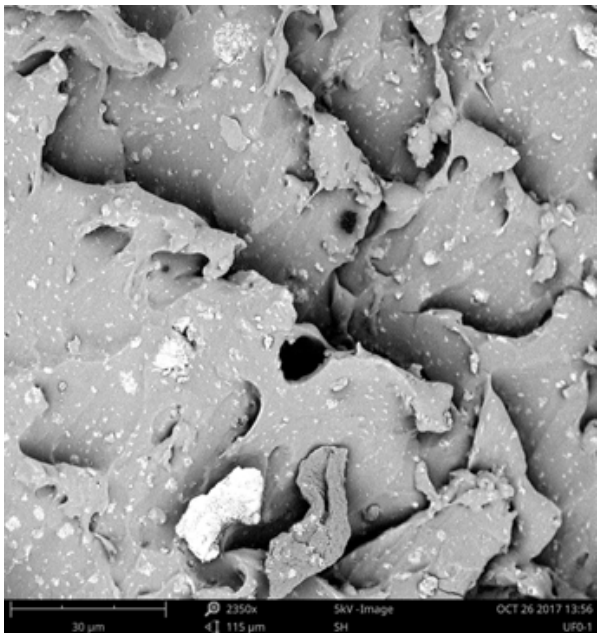

Figure 2-10 SEM image of PDMS with ZnO and CNTs hand mixed in. Aggregations appear as white bundles against a grayer matrix. This is a nonporous sample.

Using the solvent dispersion method, samples had a significantly better distribution. Specifically pictured here is a sample made using chloroform as a dispersion agent. Samples had little to no agglomerations of ZnO or CNTs. This is seen in Figure 2-11, where there are little or no "white spots" filling the nanocomposite. Instead, the overall material has a darker coloration due to a good dispersion of CNTs throughout the PDMS. Any agglomerations of ZnO are fairly small, so a reasonably good distribution has been successfully produced.

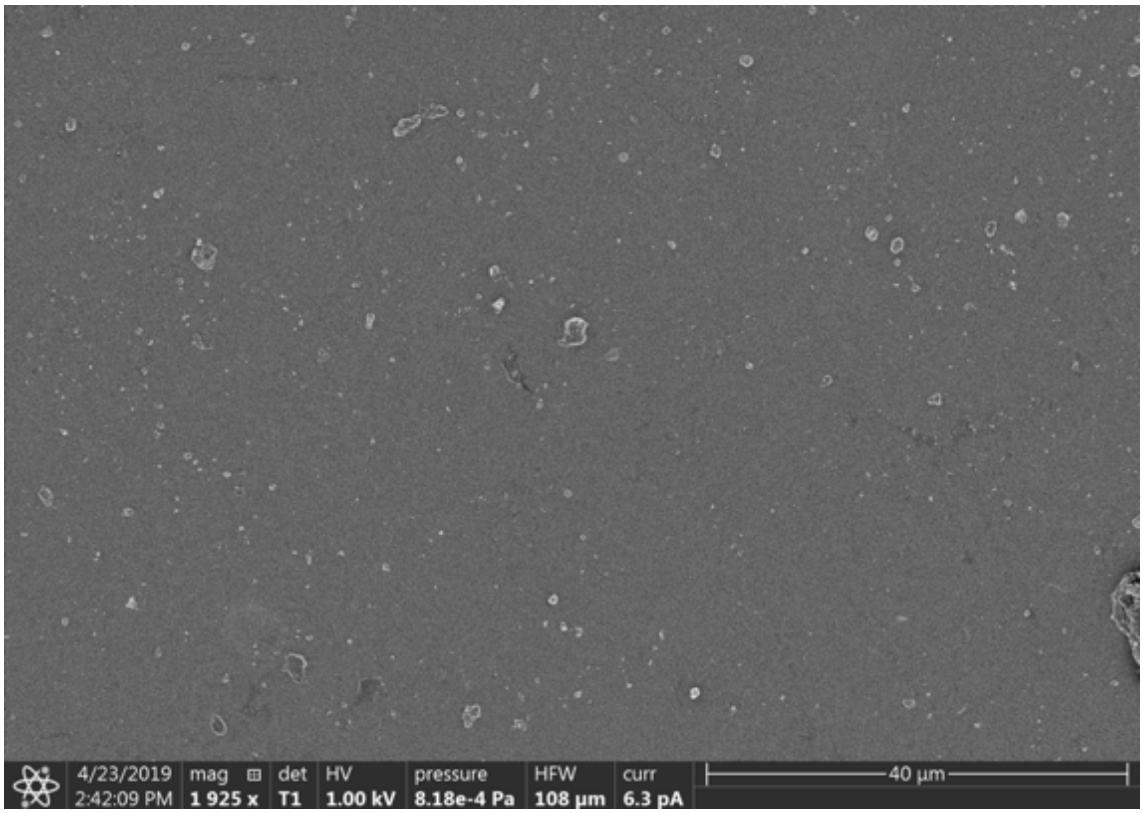

Figure 2-11 ZnO-CNT-PDMS sample produced using dispersion method. Small agglomerations can be seen, but they are not nearly as prominent as they were in the mechanical mixing method.

Additionally, during this scan, the elemental makeup of the sample was analyzed. It was determined using energy X-ray dispersive spectroscopy (EDS). In this image (Figure 2-12), the different elements are highlighted by different colors. Silicon (Si), oxygen (O), and carbon (C) are all elements found in the PDMS polymer, so it is not surprising to find these throughout the material. However, in purple, the zinc, an element not found in PDMS is dispersed throughout the sample with minimal aggregation of nanofillers compared to the hand mixed samples. This means that a uniform dispersion was achieved via this dispersion method.

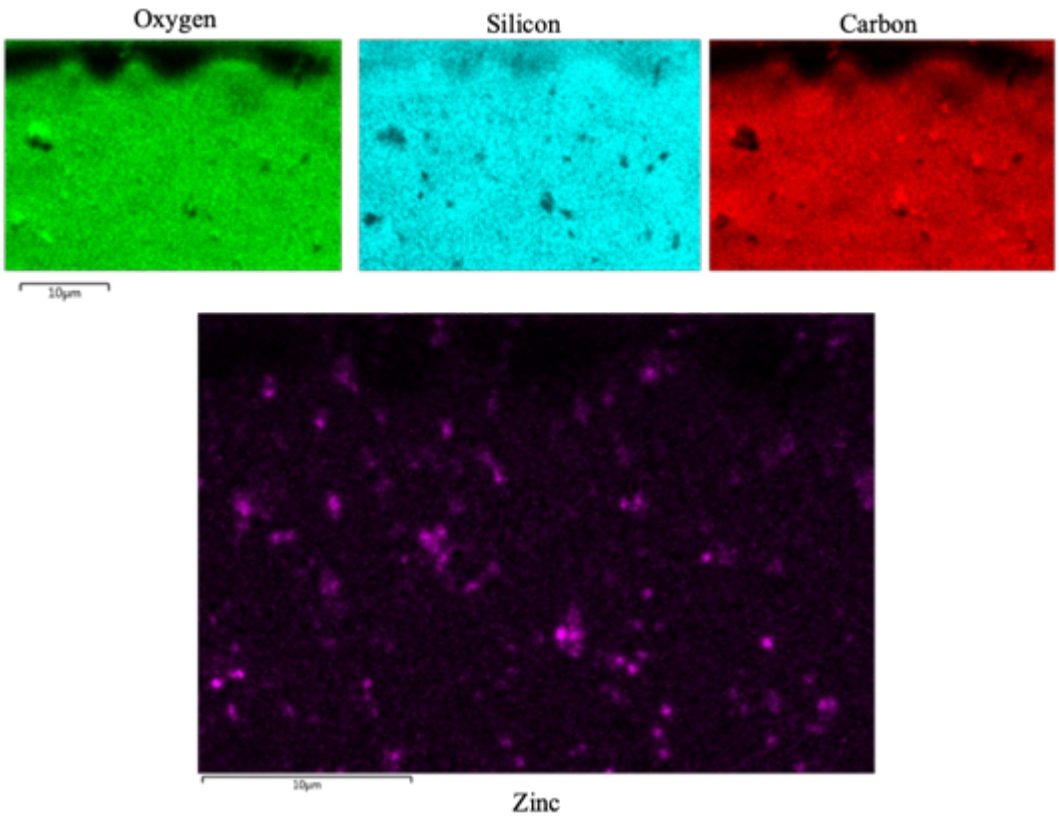

Figure 2-12 EDS Image of Elemental Dispersion. Sample fabricated with chloroform dispersion using 1% CNT, 12% ZnO, nonporous, thin film sample. Brighter colors indicate the presence of the element.

Figure 2-13 shows an SEM image of a 3% CNT sample. This image shows the structure of a typical granulated sugar sample made of 70% sugar. The sample was fabricated for tactile sensing, so it was made without ZnO. Therefore, white agglomerations do not appear in this image. However, that there are no clear aggregates of CNTs suggests a uniform dispersion of the CNTs. The shapes of the original sugar crystals are clearly seen in this image, with the throats shown in the back of several pores.

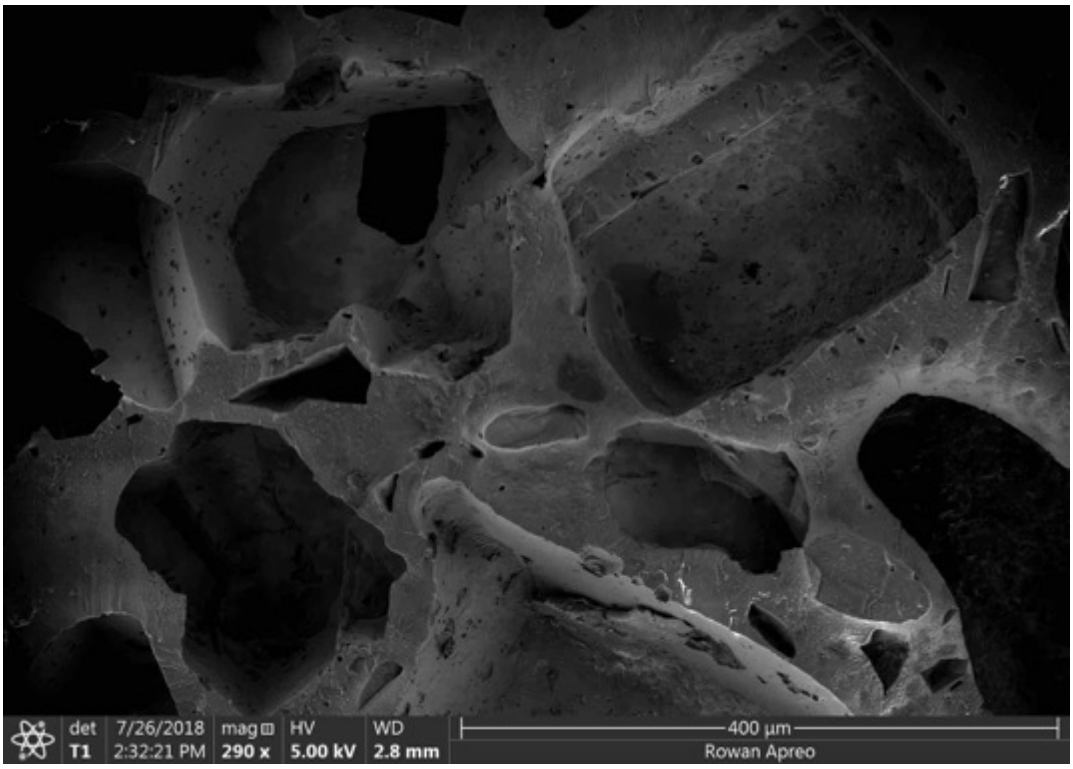

Figure 2-13 SEM Image of 3% CNTs, 0% ZnO, and 70% granulated sugar porosity in PDMS matrix. Fabricated using the dispersion method.

Figure 2-14 are images of the devices fabricated using three types of sugar that were used as scaffolding agents in the fabrication process. For ease of comparison, each image is taken of a 70% porous device. Ultrafine is shown in Figure 2-14, having the smallest pores that are the most compact. Next, a granulated sugar sample is imaged. The pores in this structure were more spaced out, though the throats are more obvious. Finally, a brown sugar sample is shown, displaying the amorphous structure of the molasses-filled sugar.

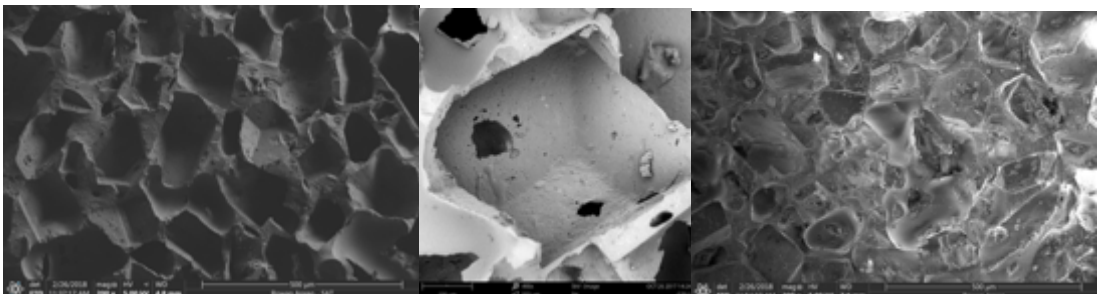

Figure 2-14 Samples made with 10% ZnO, 1% CNT, and 70% sugar; ultrafine, tessellating structure (left), granulated, clear throats (center), brown, amorphous (right). Mechanical mixing method.

2.6. Discussion of Fabrication Methods

In this section various fabrication techniques were explored in order to find the optimal method. Samples were prepared using three different types of sugar, citric acid, and sodium bicarbonate. Sugar samples had good distribution of pores for densities between 60-80% porosity. Sodium bicarbonate and citric acid both settled prior the PDMS fulling curing, causing a separation layer in the device. The results of these fabrication methods are summarized in Table 2-2. It is clear that sugar scaffolding is the most successful method for fabricating a porous structure.

Using different amounts of both citric acid and sodium bicarbonate together and partially polymerizing the PDMS, a roughly porous structure could be achieved. The two chemicals would react in the acidic acid bath while the PDMS finished the polymerization process.

This process was difficult to control on a hot plate with a petri dish, though, and samples were never functionalized mostly because they never got past an initial experimental stage. This is mostly caused by how quickly the PDMS sets during this process. Consistency of the process is difficult to achieve. If the PDMS was partially cured, the materials were effectively just another scaffold material, or worse, they

produced inconsistent pore sizes on the macro scale. If they reacted before the PDMS was ready to cure, there was no reaction occurring during the crucial curing phase and therefore no porous PDMS was produced.

Due to its unpredictable porous structure, chemical blowing was not considered as a viable option for producing either piezoresistive or piezoelectric sensors. Samples never even achieved a functional state where tests could be conducted. However, samples produced using the scaffolding method were widely successful, though sugar clearly presented itself as a superior scaffolding agent.

Table 2-2 Effectiveness of scaffolding and chemical blowing agents

Scaffolding Agent	**Successful Porosities**	**Removal Method**	**Overall Success**
Ultrafine Sugar	60-80%	Dissolved in warm water	Successful
Granulated Sugar	60-80%	Dissolved in warm water	Successful
Brown Sugar	60-80%	Dissolved in warm water	Successful
Sodium Bicarbonate	80%	Dissolved in acidic acid	Limited success
Citric Acid	N/A	Thermally decomposed	Unsuccessful

Furthermore, various techniques were studied in order to achieve a good distribution of nanomaterials in the PDMS matrix. The results of the mechanical mixing method and the dispersion method are compared in Table 2-3. The chloroform dispersion method had the best dispersion and stability; however, it used the most complicated process. Nevertheless, chloroform dispersion was used moving forward for its superior distribution and stability during fabrication. This stability is sought after because often

several samples were fabricated concurrently. Sonication of CNTs and chloroform was done for all the samples that were being produced that day, but only one petri dish can be stirred on the hot plate at a time. This caused the pre-prepared vials of CNT-chloroform to sit for several hours while other samples are being fabricated. Depending on how many samples are being made that day, it could be several hours before the last vial of chloroform/CNTs is added to the PDMS for dispersion. This stability ensured that devices fabricated later in the had the same uniform dispersion as the devices fabricated later in the day.

Table 2-3 Effectiveness of dispersion agents

Method	Ease of Use	Stability	Overall Distribution
Mechanical Mixing	Very simple, no fume hood required	N/A	Poor
IPA Dispersion	Fairly simple, requires fume hood	Poor	Good
Chloroform Dispersion	More complex, requires fume hood and training	Good	Good

Ultimately, the most reliable samples were fabricated using the sugar as a scaffolding agent and chloroform to disperse the nanomaterials. Further development of devices uses these parameters unless otherwise discussed.

Chapter 3

Mechanical Assessment of Nanocomposite Foams

3.1. Experimental

When pores are introduced to the structure of these nanocomposites, the material becomes softer, more flexible, and easier to deform. This is easiest to show by comparing the Young's modulus of the materials [51]. Lower moduli indicate softer, more ductile materials. When studying a material, this is important to understand its mechanical properties, especially when the material is being investigated for ergonomic applications. Therefore, in this paper, the Young's modulus was determined using tensile testing.

3.1.1. Tensile Testing. Tensile testing was accomplished using a SHIMPO tabletop MTS and the accompanying FGV-50XY force gauge. Prepared samples (Section 3.1.2) were clamped to the device and slowly stretched apart until they failed.

Despite the fact that these devices are used in compression, the Young's modulus of the material was calculated using tension. Since only the linear region of stress-strain curve is used for calculating Young's modulus, it does not matter whether the material is under compression or tension. This was done due to testing apparatus limitations. When enough force was applied with the SHIMPO, the machine would physically move during testing, causing a "blip" in the data. This can be seen in Figure 3-1 at around (0.04, 24).

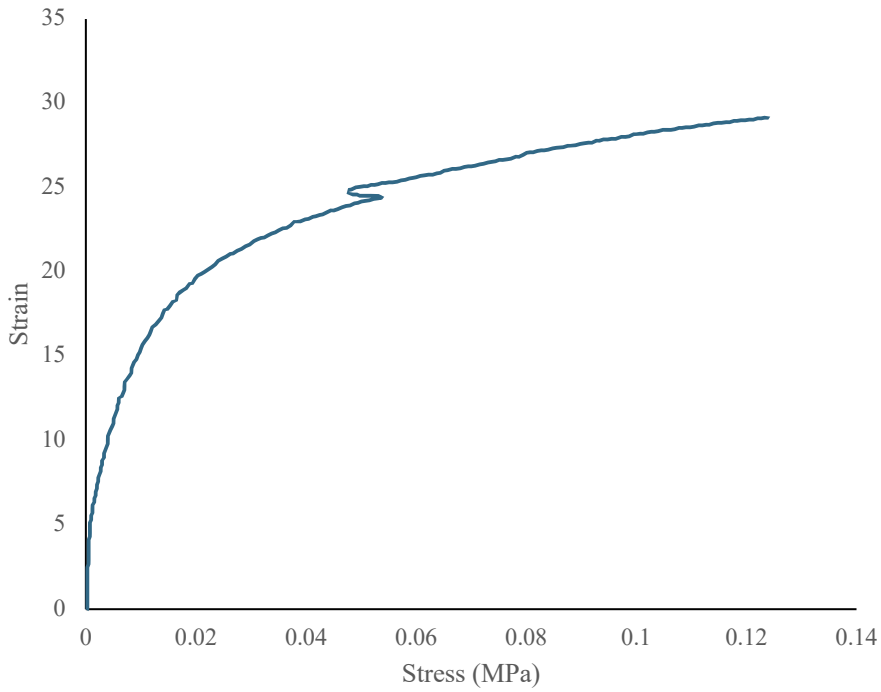

Figure 3-1 "Blip" in data during compression testing caused by machine physically moving under load.

3.1.2. Sample Preparation For tensile testing, samples were clamped into the SHIMPO MTS. However, samples could not be compressed by the clamps during testing otherwise the results would be skewed; the test would reflect mechanical properties around the deformations and stress concentrations. Instead, the ends of the sample where wrapped in duct tape in such a way that they were not being compressed. A two-part Loctite® plastic bonder was used to ensure a good bond between the sample and the tape. When the sample is put under tensile load and eventually torn, only samples that tore between the pieces of tape (and not under it) were considered. This is because if a sample tore under the tape, the testing would show the strength of the bonder/tape adherence, not the strength of the sample itself. Samples prior to test preparation are seen on the left of Figure 3-2. On the right of Figure 3-2, three samples are shown. A sample prior to testing, a sample that tore properly, and a sample that is inadmissible are pictured here.

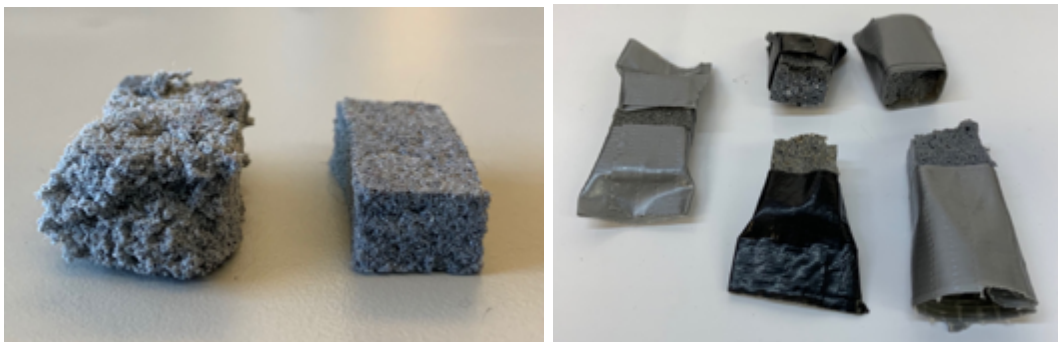

Figure 3-2 Left image, Samples prior to test preparation. Right image, from left to right, sample prepared for testing, sample that tore properly during testing, and a sample that did not tare properly.

3.1.3. Testing. Samples were mounted to the MTS and slowly pulled apart until they tore. Samples were in a completely relaxed state prior to testing, meaning the sample was not being compressed or pulled in any direction. The force gauge records the force data and the test stand records the displacement. These data are given to the computer for further processing. The computer is able to calculate the stress-strain curves for the sample based on the data provided here. This test set-up can be seen in Figure 3-3.

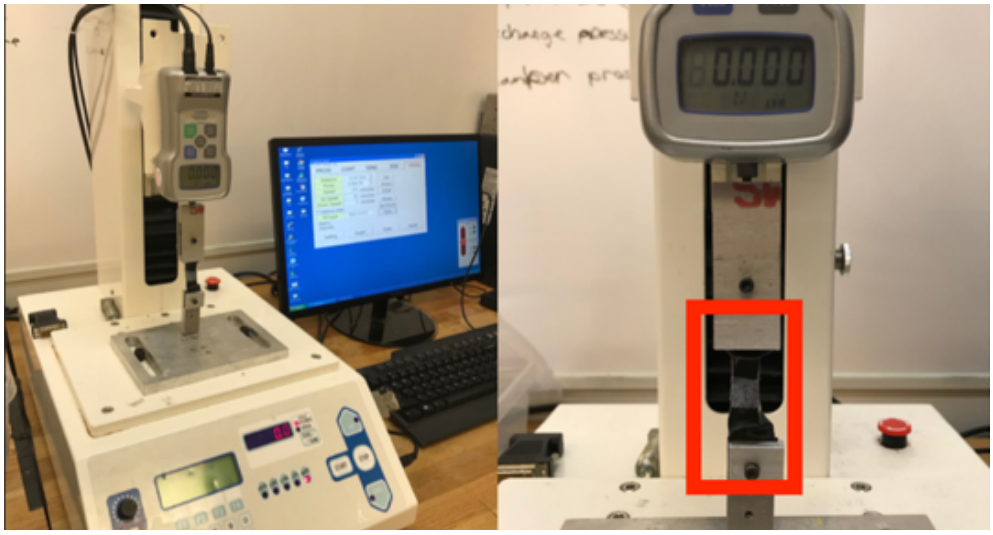

Figure 3-3 SHIMPO tabletop MTS set up. Sample under no load, prior to testing, is placed into testing set up. Duct tape wrapped around the ends provides a gripping point for the clamps that does not deform the sample.

3.2. Mechanical Testing Results

Stress-strain curves provide useful information about the Young's modulus and ultimate strength of a material. Several types of samples were fabricated using different iterations of the recipe. Three types of sugar, granulated, brown, and ultrafine, were fabricated using 60, 70, and 80% sugar for each type. The goal is to determine which type of sample will produce the most consistent Young's modulus.

3.2.1. Sugar Scaffolding Study. For Figure 3-4, 70% porous samples were made using the three types of sugar; granulated (G), ultrafine (UF), and brown (B). While several samples were tested in order to determine mechanical properties, a typical sample is plotted here to show the individual performance of each sample type. Young's modulus was calculated using the average engineering stress divided by the average engineering strain for the mostly linear region.

One of each sample is plotted to show the typical results from testing the three types of sugar. The results are plotted showing granulated sugar having the highest ultimate strength at 0.11 MPa and a Young's modulus of 0.089 MPa. Brown sugar had the lowest ultimate strength (0.056 MPa) and Young's modulus (0.027 MPa). Oddly, even though ultrafine sugar yielded the most tessellating structure of the sugars, it did not have a higher ultimate strength at 0.085 MPa or a Young's modulus of 0.048 MPa than the granulated sugar.

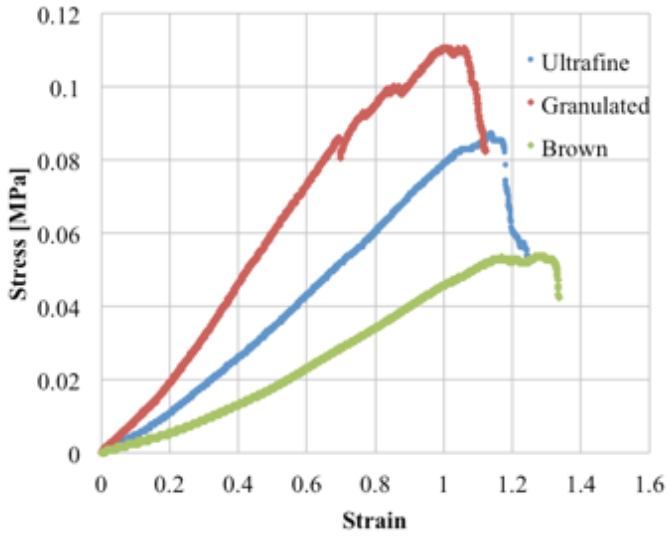

Figure 3-4 70% Porous samples with different scaffolding sugars. Ultrafine has the highest Young's modulus, brown sugar had the lowest, and granulated sugar had the mid-range.

To show the consistent behavior of the samples, three of each sample were tested and the average Young's modulus was plotted. Again, the brown sugar had the lowest average Young's modulus at 0.44 MPa and ultrafine had the highest at 0.54 MPa. Finally, the granulated sugar had a midrange Young's modulus at 0.50 MPa. There is an overlap in the standard deviation for the samples, meaning that there is not real statistical significance to the structure. However, the granulated sugar had the smallest deviation between samples which is considered important because consistent sample stiffnesses are desirable. The predictability of a device's mechanical properties is necessary for piezoresistive and piezoelectric devices, whose electrical response is directly related to the mechanical deformation in later experiments. The results of these tests are seen in Figure 3-5.

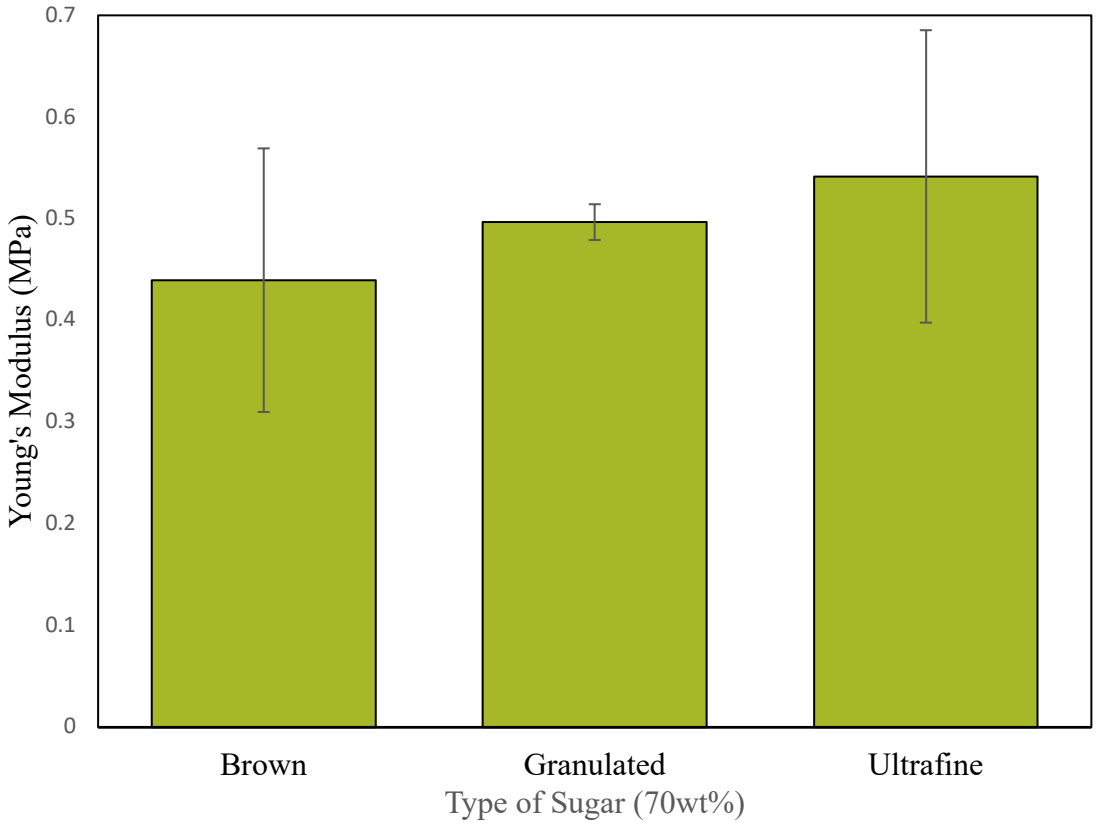

Figure 3-5 Average Young's modulus of 3 samples made with different types of sugar. Standard error bars for each sample type are included. Fabricated using mechanical mixing for simplicity.

3.2.2. Mechanical Properties of Varying Porosities. Once the optimal sugar scaffold was determined, researchers studied the effects of varying the density of the foam. This is achieved by varying different amounts of sugar scaffolding during the fabrication process. Devices fabricated with more sugar have higher porosities, meaning that they are actually less dense (more cells means more air space and less nanomaterial). Therefore, higher pore densities require less nanocomposite.

As is seen in Table 3-1, 60% porous samples use the most nanomaterials and PDMS and the least amount of sugar. Contrarily, the 80% porous sample uses the least

nanomaterials and the most amount of sugar. Because nanomaterials are more expensive than sugar, the more porous the samples are cheaper.

Table 3-1 Materials needed in fabrication of samples. Higher pore densities use more sugar but less nanomaterials and PDMS

Porosity	SOLID	60%	70%	80%
Total Materials (g)	40	40	40	40
CNTs (g)	1	0.4	0.3	0.2
ZnO (g)	4	1.6	1.2	0.8
PDMS (g)	31.82	12.73	9.54	6.36
Curing Agent (g)	3.18	1.27	0.95	0.64
Sugar (g)	0	24	28	32

Despite using less materials and being more ductile, the samples ultimate strength and Young's Modulus is lowered by the decreased amount of materials. Once the sugar scaffold has been eliminated, the porous structure is left with air filling the pores. Additionally, denser pore distribution means that each pore's stress concentrations interact frequently with one another. Interacting pore stress factors cause samples to be even more fragile while additional pores cause the wall thickness to decrease dramatically (see Figure 2-10).

As seen in Figure 3-6, samples made without pores had a Young's Modulus of 1.67 MPa, this was by far the highest. Samples made with 60% sugar had a Young's modulus of about 0.65 MPa. Samples made of 70% sugar, 0.42 MPa, and finally 80% with a Young's modulus of 0.13 MPa. Samples were also made with porosities below 60%, however, the scaffolding agent settled prior to curing and caused a layer of

separation. Therefore, while samples were fabricated for porosities between 10-50%, they were not functionalized or tested.

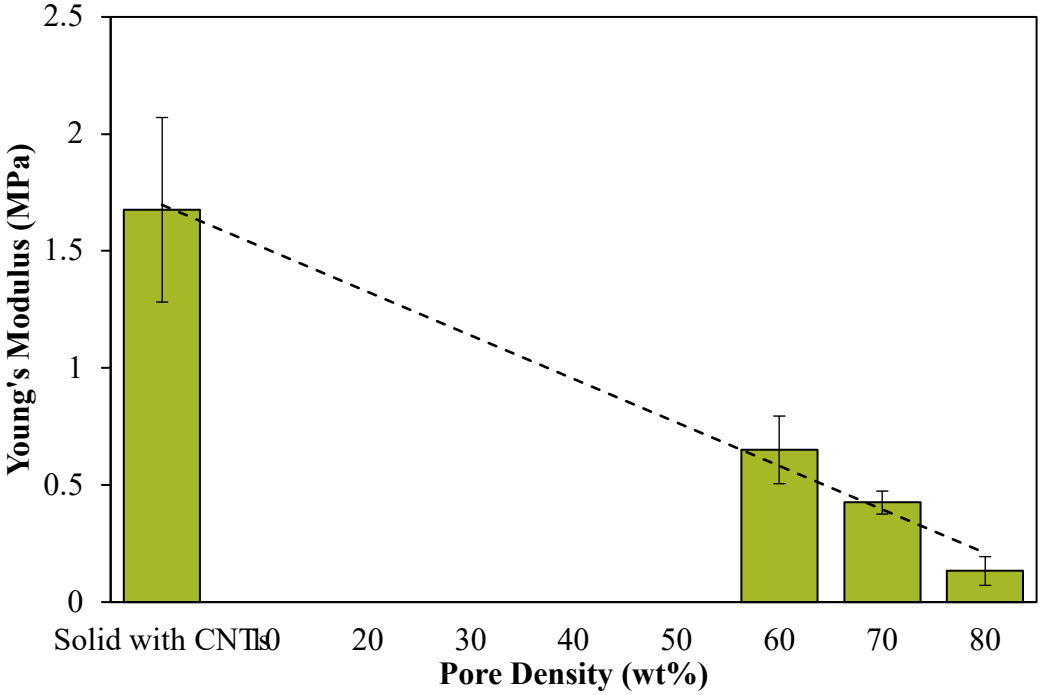

Figure 3-6 Young's modulus of porous samples, granulated sugar, chloroform dispersion. Standard error for each type sample.

3.2.3. Effects of Functionalization. To prove that CNTs actually behaved as a structural reinforcer for PDMS and not simply a fibrous mesh suspension, samples were made both with and without CNTs and their Young's moduli compared. Samples with CNTs were prepared using 3.5% CNTs and the dispersion method described earlier. In Figure 3-7, samples with and without CNTs are compared.

Samples fabricated with CNTs were stiffer than those made without, however the overlap in standard deviation means that the difference is not statistically significant.

Samples with CNTs had an average Young's modulus of 1.67 MPa while the sample made without CNTs averaged an average modulus of elasticity of 1.47 MPa.

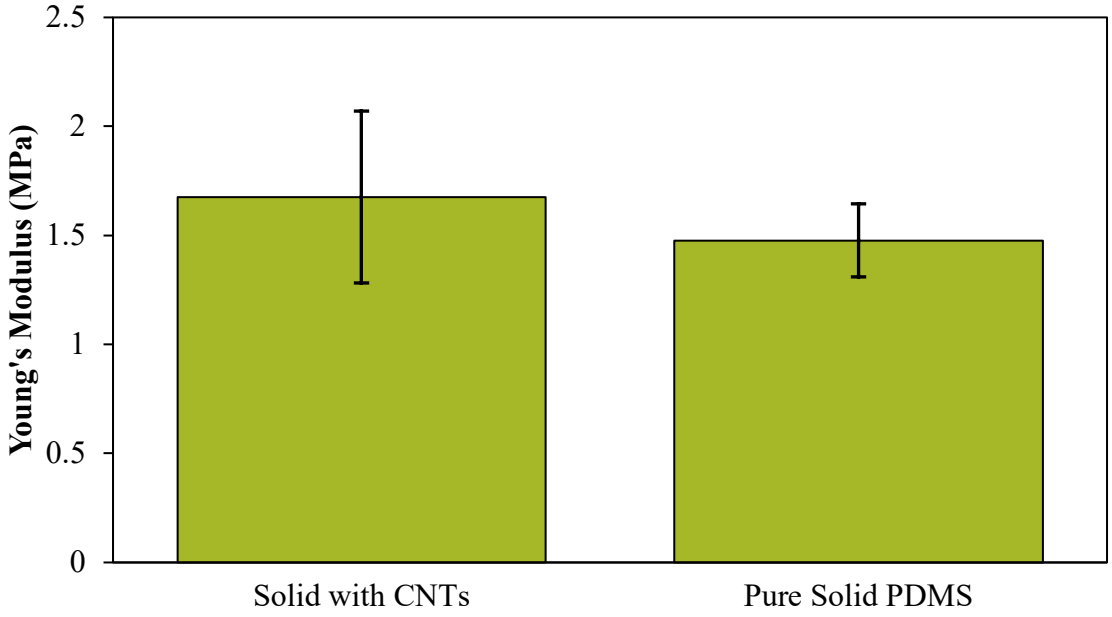

Figure 3-7 Average Young's modulus of solid samples both with and without CNTs (chloroform dispersion). Standard error for each type of sample.

3.2.4. Theoretical Density vs. Actual Density. For simplicity during fabrication, the percentage that is referred to in this text is the weight percent (wt%). Materials are weighed out on a scale during fabrication, providing a weight for the overall samples. However, porosity is a measure of volume, not mass. So, when a sample is made with "60wt%" its actual porosity might be slightly different.

To account for this, samples were weighed before and after the sugar was removed in order to determine their actual density (in g/cm^3). As expected, solid samples

were the densest at 0.899 g/cm^3. On the other hand, the 80% porous samples were 0.217 g/cm^3 which is the lightest. Figure 3-8 displays these data.

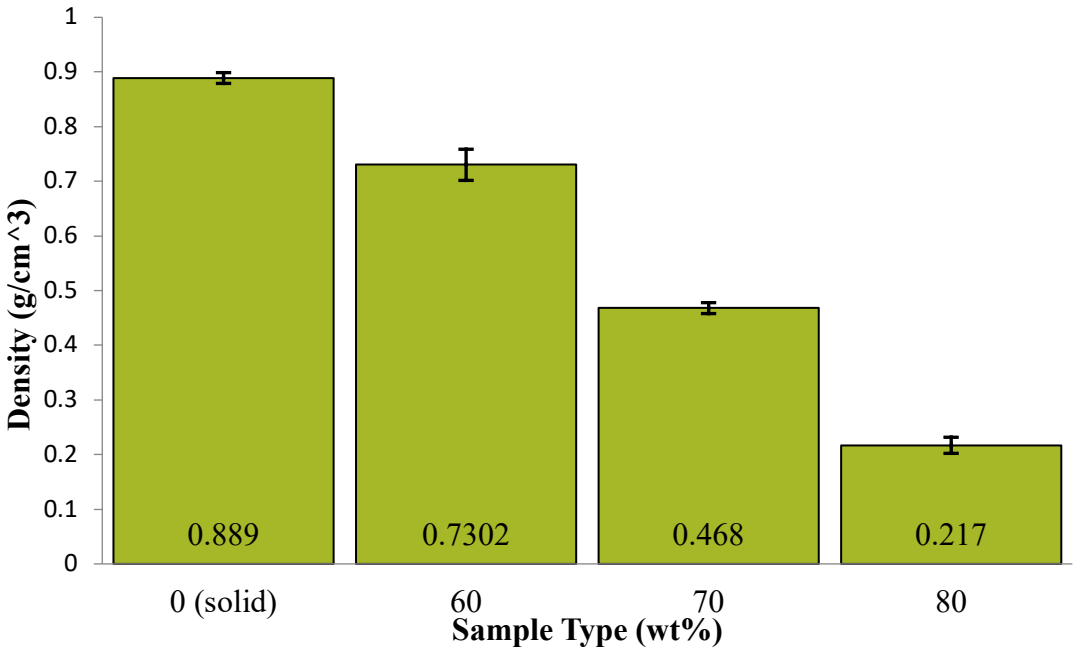

Figure 3-8 Density of Samples vs wt%. Standard error for each sample type, chloroform dispersion.

3.3. Discussion of Results

After experimenting with different the sugars, granulated sugar was deemed the best sugar scaffold. It had the most predicable Young's modulus and the easiest fabrication. This was due in part to the larger pores of granulated sugar and throats interconnecting (compared to the ultrafine samples that required hours, sometimes days to completely dissolve sugar due to the lack of good throats between ultrafine sugar pores). On the other hand, brown sugar is made of up to 10% molasses and the rest just

white granulated sugar. By adding molasses to the granulated sugar, it takes the brown sugar days to dissolve even in warm water bath and a stir bar. The water needed to be changed the most frequently, every 4-6 hours for 3-4 days. However, the granulated sugar samples could be left overnight in a warm water bath (90°C) and all the sugar would be dissolved by morning in a single water bath.

The granulated sugar also had the most consistent mechanical properties. The deviation sample-to-sample was smallest when compared to the other porosities. As it was stated before, samples need to be mechanically predictable for sensor application. Therefore, the 70% porosity samples with the most predicable mechanical properties were considered optimal.

Using the information from these studies, devices fabricated using granulated sugar at 70% porosity were the easiest to fabricate. Therefore, the team proceeded in making granulated sugar samples at this porosity. The results of these tests prove that the tuning the mechanical properties of PDMS nanocomposites is a viable option. Devices were fabricated and tested using the three types of sugar. Samples made with more sugar were ultimately softer and more ductile than the samples made without sugar. By changing the sugar that is used, the density at which it is used, and adding nanomaterials, mechanical properties like the ductility of the sample can be changed. Furthermore, the addition of a nanomaterial filler effects the mechanical properties of the matrix. Therefore, devices were made and fabricated both with and without CNTs. Ultimately, it was determined that CNTs behave as a structural reinforcer for PDMS, making the material stiffer during tensile testing.

Different densities of pores were also studied in this experiment. Samples made with 0, 60%, 70%, and 80% scaffolding material were fabricated. Again, the devices with the most consistent results were considered the most successful. This turned out to be the granulated sugar 70% porous device.

Chapter 4

Pressure Sensitivity of CNT-functionalized PDMS

4.1. Flexible and Porous Pressure Sensors

In this paper, pressure sensors were produced using PDMS and CNTs. By manipulating the concentration of both pores and CNTs in the samples, a correlation can be drawn between these properties and the piezoresistivity of the sample. Each variation of the tactile sensors behaved as expected within a certain range of pressures. These promising results show usefulness in pressure sensing.

4.2. Preparation of Tactile Sensors

For this set of experiments, samples were prepared as tactile sensors relying on piezoresistivity. During this study, the amount (%) of CNTs are to make the samples was varied from 1% to 5% CNTs at 0.5% intervals (0.5%, 1.0%, 1.5%, etc.). For these experiments, the dispersion method is used to make sure that CNTs are well distributed throughout the sensors. The dispersion agent chosen was chloroform since it yielded the most stable solution of CNTs during the fabrication process, as was discussed in Section 2.2.2.

Using these methods, devices were fabricated using the materials outlined in Table 4-1. This recipe will make about six ½" × ½" × ¼" pressure sensors with 70% sugar.

Table 4-1 Materials needed to fabricate 70% porous devices with different concentrations of CNTs, produces ~6 pressure sensors.

Required Materials	**0.5%**	**1%**	**1.5%**	**2%**	**2.5%**	**3%**	**3.5%**	**4%**	**4.5%**	**5%**
CNTs, 0.4 mg/mL	0.68	0.68	0.68	0.68	0.68	0.68	0.68	0.68	0.68	0.68
PDMS, 0.13 g/mL	135.32	67.32	44.65	33.32	26.52	21.99	18.75	16.32	14.43	12.92
Curing Agent	13.53	6.73	4.47	3.33	2.65	2.20	1.87	1.63	1.44	1.29
Sugar	348.91	174.37	116.20	87.11	69.65	58.02	49.71	43.47	38.63	34.75

4.3. Electrical Resistance Testing

In order to better understand how these sensors behave under load, samples were mechanically compressed while their electrical properties were being evaluated and recorded. Samples were compressed as seen in Figure 4-1 and Figure 4-2.

Data were collected using the SHIMPO MTS again, however, instead of tensile testing, here, samples were compressed with the device while their electrical response was tracked. The blip mentioned earlier does not affect the outcome of these tests because Young's modulus was not calculated. Since the compression test uses known force outputs, the blip is irrelevant.

The electrodes were connected to the top and bottom of the sensor, making a sandwich-like test setup. Samples were placed on top of a copper electrode with another copper electrode on top. This allowed full contact with both the top and bottom of the pressure sensor fully and therefore accurate readings from the source meter as the pressure sensor is deformed. Each electrode was connected to the multimeter, forcing a known voltage (20 V) through the sample. The set-up is shown as a schematic in Figure 4-1 and in a photograph in Figure 4-2.

Sensitivity is determined by each sample's electrical response to mechanical compression. Once contact between the compression surface and the pressure sensor is made, the current is measured and compared to the pressure being applied. In order to ensure that a solid contact is made between the sample and the compression surface, measurements are started at 2 N of force. Then, at 2 N increments, the pressure is increased until the current readings plateau and applying additional pressure no longer changes the electrical properties of the sample.

The devices had very high resistances, so the best way to determine the resistance was to track the change in current of the sample as it is deformed by the SHIMPO tabletop tester. Using Ohm's law (V=IR), a resistance for every sample at each step could be calculated. Current values were recorded at 2, 4, 6 etc. up to 20 newtons and converted to resistance.

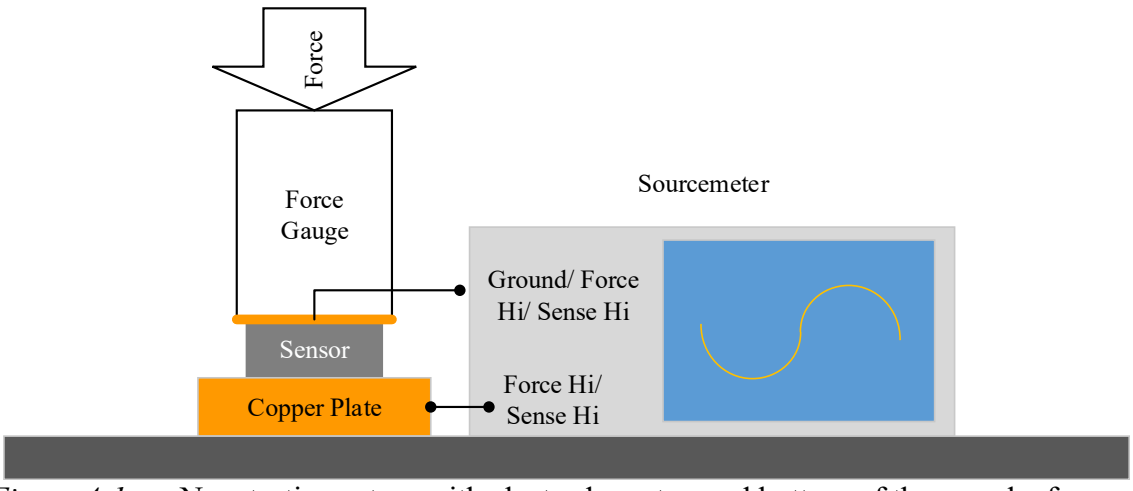

Figure 4-1 New testing set up with electrode on top and bottom of the sample, force is applied and distributed equally over the sample.

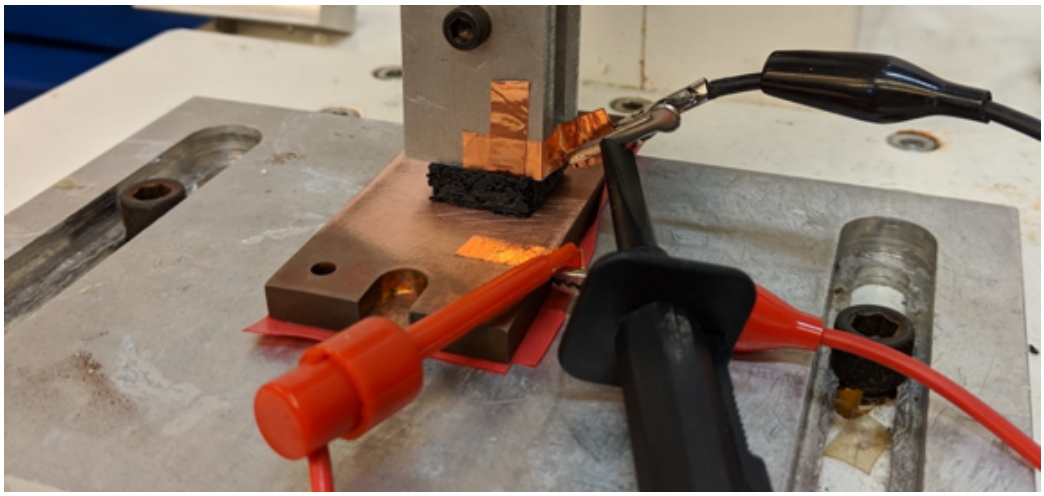

Figure 4-2 Sandwich structure for testing tactile sensors. Copper tabs allow alligator clips a better place to grip. Copper plate required sanding between tests to maintain a clean surface.

4.4. Results of Electrical Resistance Testing

In order to quantify the sample's sensitivity, the change in resistance was compared to the initial resistance (at 2 N of pressure). This gives a ΔR/R graph (change in resistance divided by the resistance), also known as the sensitivity of the sample. Samples of various pore densities were studied in this experiment in order to determine if the porous structure of the tactile sensors would affect the samples ability to perform as a sensor. It is clear that the sensitivity drops as the porosity is increased, however, the drop is not very significant, and the samples are still sensitive enough to detect pressures up to 16 N, though some were able to detect pressure accurately to 20 N.

To quantify the data collected, the average resistance at each time step was taken. About 1 minute at each time step was collected, but only about 30s of data was used for to calculate the average at each time step. This average is divided by the average initial resistance. Equation 2 shows how this is achieved.

$$\frac{\Delta R}{R}(\%) = \frac{(Average\ \ \Omega)\ at\ (N_x)}{(Average\ \Omega\ at\ (N_1)} \quad [2]$$

Figure 4-3 is an example of the typical resistances as pressure is applied. Represented here is a 4% CNT sample's resistance is traced as the sample is put under load in 2 N increments (shown by the "jumps"). These jumps indicate where the machine was moving, the average was taken after the force was steady to make sure that data was accurate. In order to show the change in pressure, how much pressure being applied at the time that the resistance is measured.

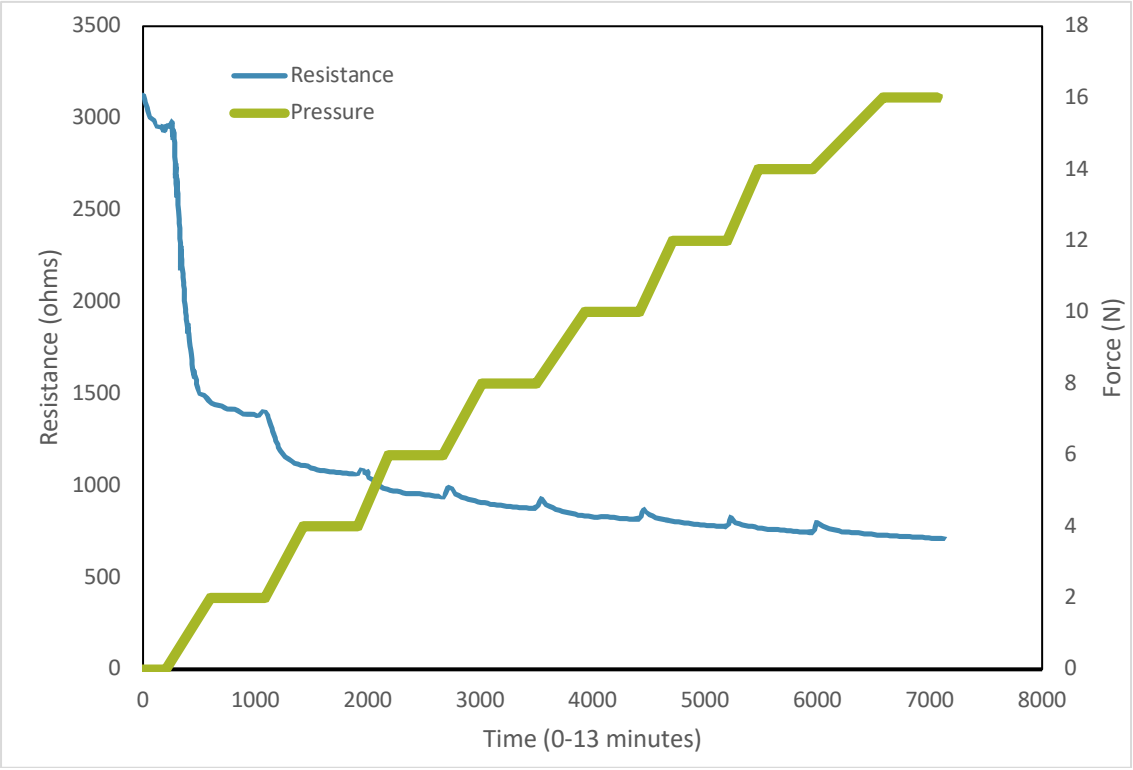

Figure 4-3 Typical resistance values while sample is under load. As pressure increases, resistance decreases.

Using the information produced by these graphs, the average resistance was compared to the initial resistance (at 2 N) and the change in resistance was plotted against the force. In Figure 4-4 the results of comparing different CNT concentrations is displayed. 2%, 3%, 4%, and 5% CNT concentrations were compared for performance.

For these set of experiments, multiple samples of each type were measured, and their values averaged together to produce data like in Figure 4-4. 3-5 samples of each iteration of the experiment were used for testing. From these tests, researchers were able to conclude that the 5% CNT samples were the least sensitive while the 3% CNT samples had the highest sensitivity.

This is due to the connectivity between the CNTs as the sample are compressed. When the concentration is higher, too much electricity flows through the CNTs when the sample is compressed, limiting the sensitivity. In the same manner, not having enough CNTs would not allow electricity to flow, making the lower CNT concentration samples too insulating to be sensitive. This was the case with the 1% samples which could not produce meaningful data on the pressure. For this reason, they are not represented in the figure. However, the 2%, 3% and 4% samples all showed sensitivity for pressures up to 12 N.

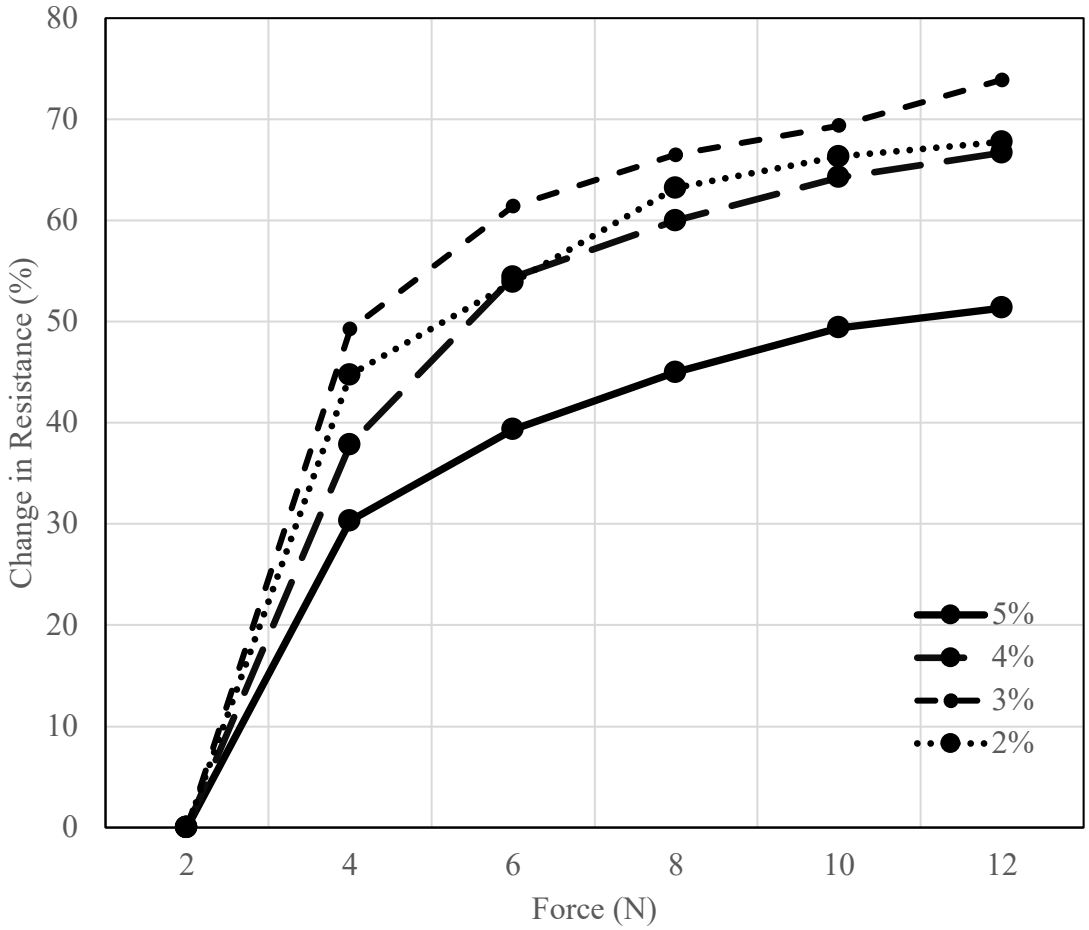

Figure 4-4 CNT Concentration Study. Devices made with higher CNT concentrations (5%) and lower CNT concentrations (1%) Mid-range CNT concentrations displayed sensitivity between 2-12 N.

After determining that there is a relationship between sensitivity and CNT concentration, the sensitivity at a specific pressure is compared for each iteration of the device. Samples were made using 1.0% CNTs, 1.5% CNTs, 2.0%, etc. up to 5% CNTs concentration. The results can be seen in Figure 4-5 where the average resistance at 6 N is plotted for each concentration of CNTs. The lower CNT concentration samples (below 3%) had significantly higher resistances than those above 3.5% CNT. This "drop off" in the resistance (marked by the dotted line) marks a dramatic shift in the electrical

conductance of the PDMS/CNT sensors. At around 3% CNTs and lower, the CNTs are too dispersed to connect with each other when the sample is compressed. Alternatively, the samples with 5% CNTs had strong contact between the CNTs even when no pressure was applied, so they did not change resistance as much when the sample is compressed. The 3.5-4.5% CNT devices all had similar sensitivities. Since a goal of this project is to minimize material usage and costs, the 3.5% CNT sample using the least amount of materials is ideal.

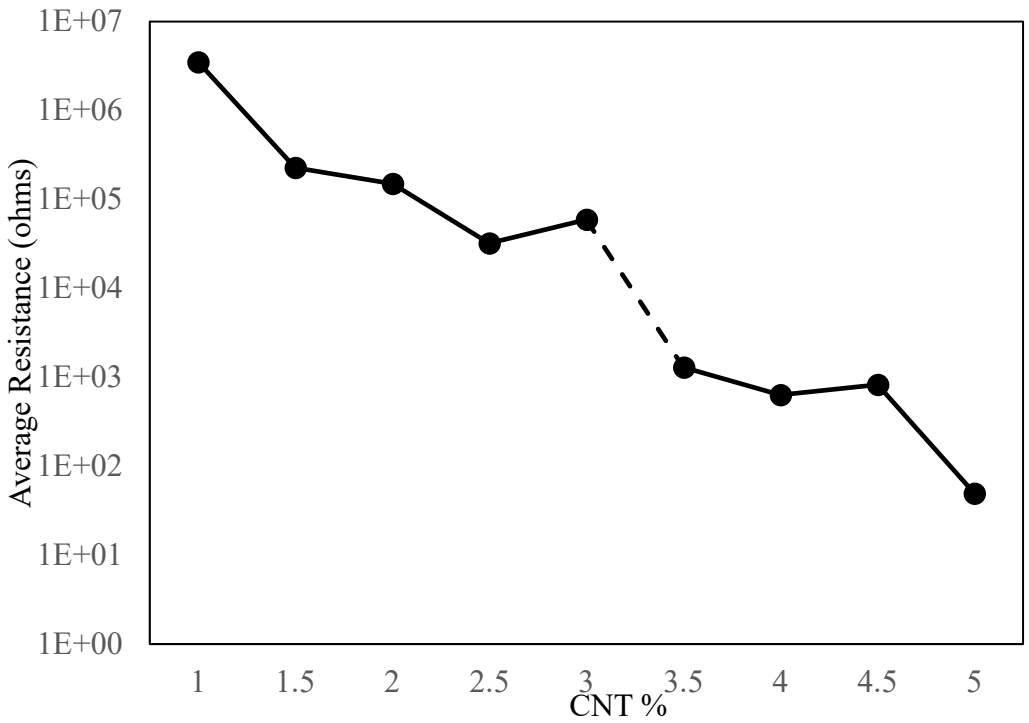

Figure 4-5 Average Resistance at 6 N for different CNT concentration samples. Samples made with less than 3% CNTs had very high resistances, samples made with 3.5-4.5% CNTs were considerably more conductive. Samples made with 5% CNTs had significantly lower resistances but were not very sensitive. A steep decrease in resistances between 3-3.5% CNT shows a critical mass for conductance.

4.5. Effects of Porosity on Sensitivity

After determining that 3.5% CNT concentration was optimal, the effects of varying the porosity could be explored more fully. Adding CNTs makes PDMS sensitive but they also stiffens the PDMS. Samples were fabricated 60% porous samples, 70% porous samples, 80% porous samples, and as non-porous bulk samples. Based on previous research, the granulated sugar would provide the most consistent results, therefore sensors were fabricated using the granulated sugar. Similar to the CNT concentration study, samples were placed on the SHIMPO machine and compressed. The current was recorded and using ohm's law, and again, the resistance was calculated.

The results of this study are shown in Figure 4-6, where the average change in resistance is plotted against the initial resistance. Again, 3-5 samples were tested, and the average resistance of each sample was quantified.

In this test, the solid samples showed the highest change in resistance, making them the most sensitive. The 60%, 70%, and 80% porous samples were progressively less sensitive the more porous they were, which signifies that by using a porous structure does sacrifice the sensitivity of a device to a degree. However, the difference is minimal, and the sensors were still able to detect pressures up to 16 N.

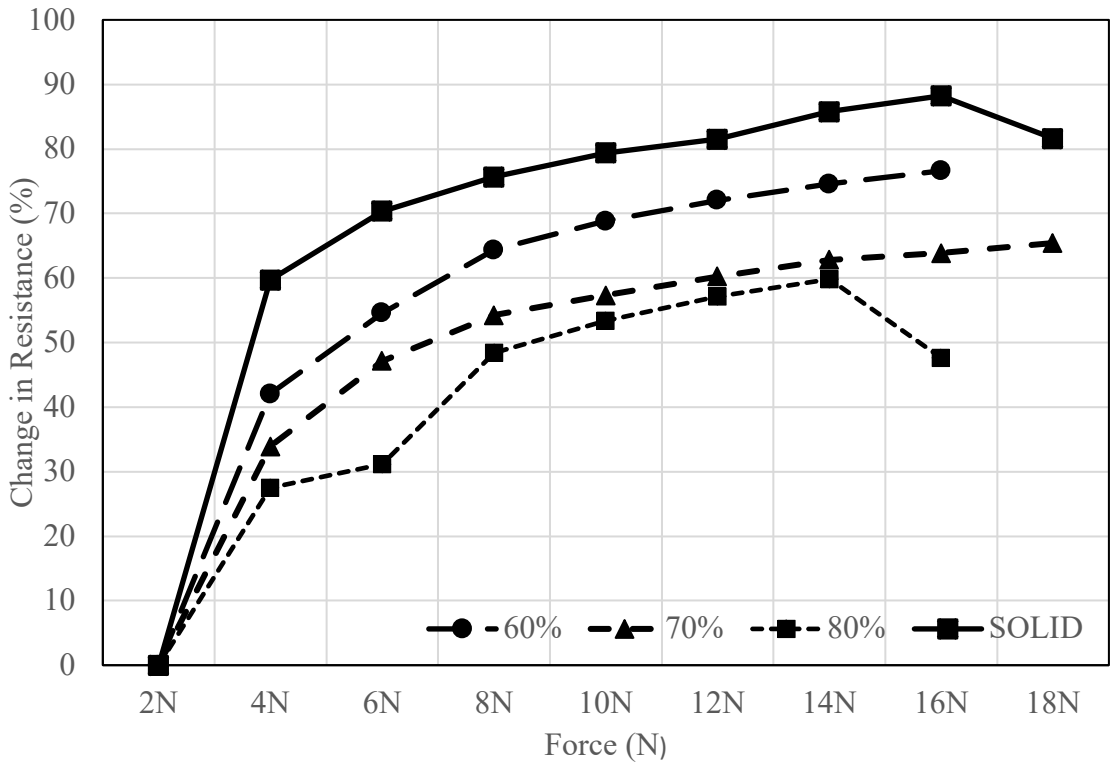

Figure 4-6 Average resistance of various porosity samples as pressure is applied. More porous devices were less sensitive, with 80% porosity showing irregular changes in resistance.

These results are promising because adding pores to the structure of the sensors does not dramatically affect their sensitivity. The porous structure makes the sensor more ductile and easier to deform than the solid sensors. Additionally, the use of sugar as a scaffold means that less nanomaterials needed to produce samples (compared to the solid samples). This makes the porous sensors less expensive than their solid counterparts.

Similar to how the CNT concentration study was done, the effects of adding pores was studied to compare sensitivity at a specific pressure. The average change in resistance at 10 N was compared for the four sample types; solid, 60%, 70%, and 80%. As the porosity increases, the average change in resistance decreases for each pressure step. The 80% porous sample had the lowest change in resistance compared to the 60%

and 70% sensors. 70% was less sensitive than 60%, and the solid samples had the largest change in resistance at 10 N. This can be seen in Figure 4-7.

In these experiments, 80% porous samples experienced an average of 51% decrease in resistance at 10 N. The 70% porous sample experienced a 57% decrease in resistivity. At 6 N, the 60% porous sample experienced a 68% decrease in resistivity. Finally, the solid samples had the greatest change in resistance at 79% decrease. Because earlier studies showed that pore densities under 60% had separation during the curing process, lower pore densities were not studied for this set of experiments. The results of this test show that solid samples had were the most sensitive, however, the porous samples were not significantly less sensitive. Porous structures are still a viable option moving forward for tactile sensors.

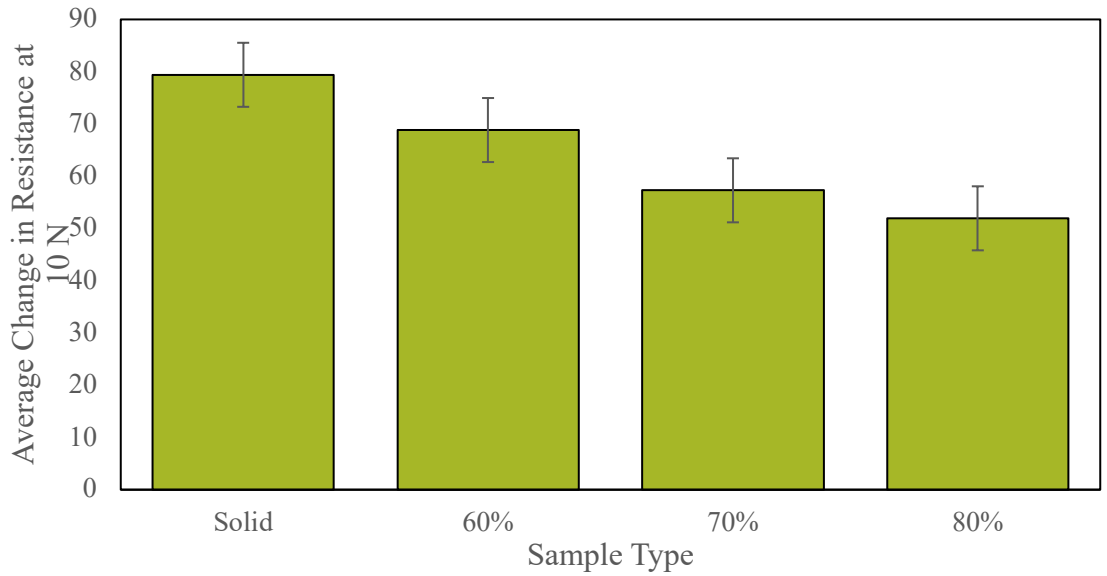

Figure 4-7 Average change in resistance at 10 N for different porosity samples. More porous samples were less sensitive

4.6. Discussion of CNT and Pore Concentration Study

Using the data gathered in this set of tests, the optimal CNT concentration is determined. Samples starting with as low as 1% CNTs were tested and up to concentrations as high as 5% were tested to quantify their sensitivity. At either end of the spectrum, sample performance is limited and unreliable, however, the mid-range concentrations were optimal for tactile sensing.

1% samples had the highest resistance because they are the most insulating (they have the least amount of CNTs). The small amount of CNTs leaves a large distance between CNTs in the composite. Even when the sample is compressed, the CNTs are not in close enough proximity for good electrical conductivity. This makes the change in resistance smaller, meaning samples are not very sensitive. 5% CNT samples experienced the opposite: they were so conductive because the CNTs already have good contact prior to compression. This makes the resistance very low. As the sensor is compressed, the amount of connected CNTs does not change much, so the device not only very stiff but also not very sensitive.

The midrange concentrations of CNTs were sensitive enough to pick up a wider range of pressure. The 3.5% samples had a larger change in resistance than the lower CNT concentrations. This makes the 3.5% CNT sensors more sensitive than the <3.0%.

Different pore densities were investigated in order to determine if there was a significant effect on the device's functionality with a porous structure. 0, 60, 70, and 80% porous sensors were studied. A porous structure does slightly degrade the devices sensitivity; however, sensors were still capable of detecting pressures accurately.

The results of the CNT concentration results compare to the results found in several studies [1, 51, 59]. More than 10% CNT is almost never used, though concentrations usually are between 1-5%. On the other hand, [51] reported more sensitivity from their more porous samples. These devices were tested under both small and large strains, while the investigation of this thesis focuses on compressive loads for pressure sensors.

Chapter 5

Energy Harvesters and Piezoelectric Nanocomposite Devices

5.1. Development of Piezoelectric Nanocomposite

In this chapter, ZnO and CNTs form the nanocomposite and functionalize the PDMS to a piezoelectric device. Piezoelectric devices made of ZnO, CNTs, and PDMS have been fabricated as thin films and bulk porous samples. The thin films were fabricated using a spin coating technique while the bulk porous samples were prepared using the same methods described in earlier sections. It is believed that a bulk sample would produce higher energy outputs than a thin film due to the increased distance that the material is able to deform. However, PDMS blocks are much stiffer than the thin films. To combat this, a porous structure is utilized to make samples more deformable. Porous structures, as discussed earlier, make the material softer and more pliable. This makes them more durable and flexible. Sensors made with porous structures are lighter and more flexible. Additionally, the porous structure reduces the physical number of nanomaterials needed to produce samples compared to solid bulk. This effectively reduces the costs associated with nanomaterials by making samples with up to 80% sugar.

5.2. Fabrication of Thin Film Piezoelectric Device

In this paper, both porous and thin film piezoelectric sensors and energy harvesters were fabricated. Samples were created using both a thin film technique and the scaffolding technique. For a thorough investigation, the three different types of sugar are used at various pore densities for optimal power output. These were compared to the thin film samples.

A few research papers have made piezoelectric devices using ZnO and CNTs [13, 63, 64, 71]. In this set of experiments, thin film devices are fabricated using a common lab practice, spin coating. Many of these papers utilized mechanical mixing techniques, however we know that a better dispersion occurs when dispersion techniques are used. Therefore, for this project, thin film samples were produced using chloroform dispersion.

In order to mix in the ZnO, it was mixed into the PDMS after the CNT/chloroform solution is added, but before all of the chloroform has evaporated out. Once all of the dissolvent is boiled out of the PDMS, the heat is turned off, but the stir bar is still used to keep stirring the nanocomposite (~60rpm). This keeps the ZnO and CNTs from settling as the PDMS cools off. The curing agent is added to the (cooled to room temperature) PDMS and mixed well by hand. The nanocomposite is then de-bubbled in a vacuum (center, Figure 5-1).

To achieve thin film piezoelectric devices, the uncured nanocomposite is spun onto a 2" × 3" glass slide at 500 rpm for 60 s and then speed is increased up to 1500 rpm for another 30 subsequent seconds. A second layer is applied and spun at the same parameters. After the second layer is spun, the device is cured on a hot plate for approximately 4 hours at 90°C. The resultant film can then be peeled off the slide, leaving a thin film around 0.1778 mm thick. Figure 5-2 shows the fabrication process of this type of sample.

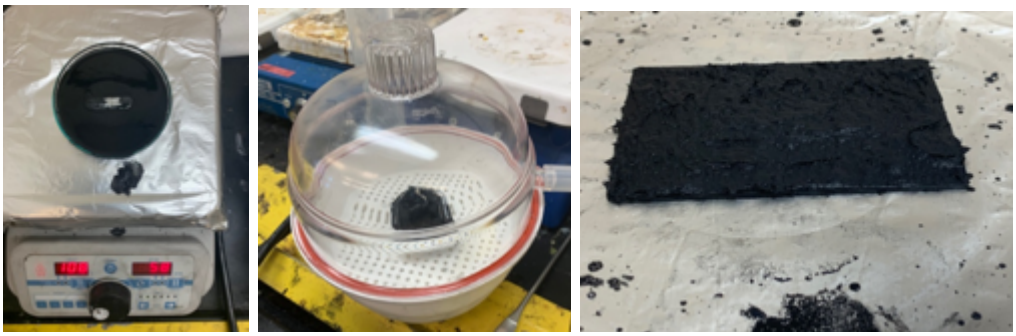

Figure 5-1 Thin film sample in various stages of preparation. Left, CNTs, PDMS, ZnO and chloroform. Middle, CNTs, ZnO, and PDMS in de-bubbler. Right, thin film being cured.

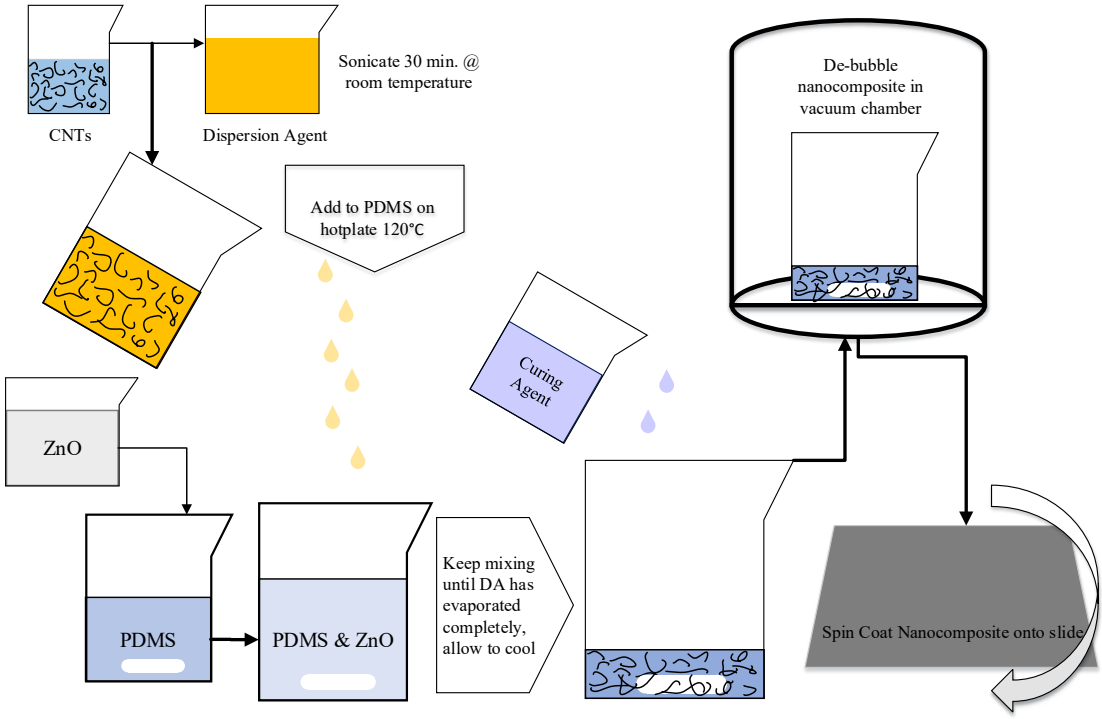

Figure 5-2 Fabrication flow of thin film samples. CNTs are ultrasonicated in chloroform for 30 minutes at room temp. CNT/chloroform suspension added to PDMS on hot plate. ZnO is mixed into composite. Composite is stirred with a magnetic stir bar until all the chloroform has evaporated. Composite is allowed to cool to room temp. Curing agent is mixed in and entire solution is degassed (~30 minutes). Nanocomposite is poured over a glass slide and spun at 500 rpm for 60 seconds and then 1500 rpm for an additional thirty seconds. Two coats are applied, and sample is finally cured on a hot plate at 90°C for 4 hours.

5.3. Fabrication of Porous Piezoelectric Devices

Fabricating large, porous samples was the base for further research because these thin film devices are delicate, hard to peal, and not easily mass producible. Instead, a porous structure is proposed for scalability and ease of fabrication.

Devices for this process were made using the mechanical mixing techniques from above. Originally thin film devices were not studied, and neither were the dispersion techniques. The devices were produced using the same simple methods described in [63]. However, instead of spin coating, samples were produced in bulk using the molds pictures earlier. Table 5-1 shows the amount of each ingredient that went into producing the piezoelectric foam devices. This table shows how the more porous sensors required less PDMS, less ZnO, and less CNTs than the solid devices.

These foamed devices were made using the sugar scaffolding method described in earlier chapters. These pore structures are made from granulated sugar for the ease of fabrication and optimal mechanical properties, a decision based on the extensive research mentioned up to this point.

Table 5-1 Materials used in fabrication of porous samples.

Porosity	SOLID	60%	70%	80%
CNT Concentration	2.5%	2.5%	2.5%	2.5%
Total Materials (g)	40	40	40	40
CNTs (g)	1	0.4	0.3	0.2
ZnO (g)	4	1.6	1.2	0.8
PDMS (g)	31.82	12.73	9.54	6.36
Curing Agent (g)	3.18	1.27	0.95	0.64
Chloroform (mL)	85	85	85	85
Sugar (g)	0	24	28	32

5.4. Dipole Alignment of Thin Film and Porous Devices

In order to optimize the electrical output of devices, a strong electrical current is supplied to the device so that it can undergo dipole alignment.

5.4.1. Dipole Alignment Setup. The parameters that were chosen for dipole alignment on thin-film samples were 1.7 kV at 150°C for 12 hrs. The voltage was calculated using the thickness of the thin-film samples after they were peeled off the glass slide. The sample was then sandwiched between the copper plates with pure-nonfunctional PDMS cast over top as a dielectric layer, seen on the right of Figure 5-3. For foam samples that underwent dipole alignment, the middle photograph of the same figure shows the thicker rubber dielectric layer that was inserted between the copper plates (no pure-PDMS was cast on the copper for these samples). These samples were also poled at 150°C for 12 hrs similar to what was done in [22, 70, 71]. However, foam samples were significantly thicker than the thin film samples. As a result, the poling voltages that were tested were 6, 8, and 12 kV.

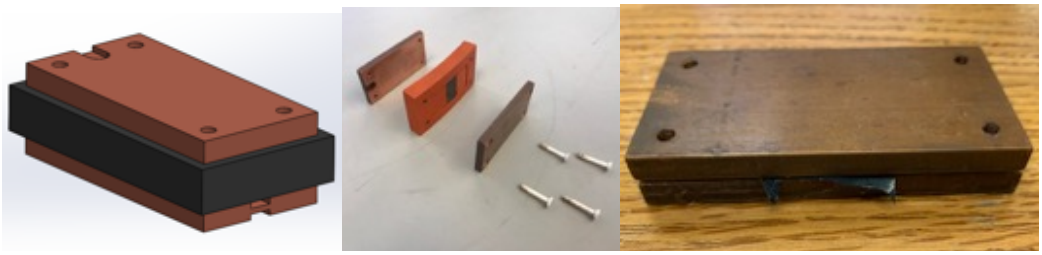

Figure 5-3 Parallel Capacitor Plate Set-up (CAD drawing, left; foamed sample set up, middle; thin film set-up, right).

5.4.2. Safety enclosure for dipole alignment. During the poling process, high voltages were used to align the dipoles of piezoelectric particles. Because this research is done in a public university in a lab frequented by non-lab personnel, a safety enclosure was created to keep high-voltage contained during the 12-48 hr. process of dipole alignment. This was done using a safety enclosure fabricated of insulating materials. The enclosure was large enough to cover the entire hot plate during poling. A simple box made of G-11 garolite with acrylic windows served this purpose.

Figure 5-4 shows the device being used over the hot plate. This basic design kept unknowing passers-by from accidently electrocuting themselves. The lead wires for the power supply go into two holes drilled into the either side of the box. The hot wire and the ground wire each connect via alligator clips to one of two copper capacitor plates.

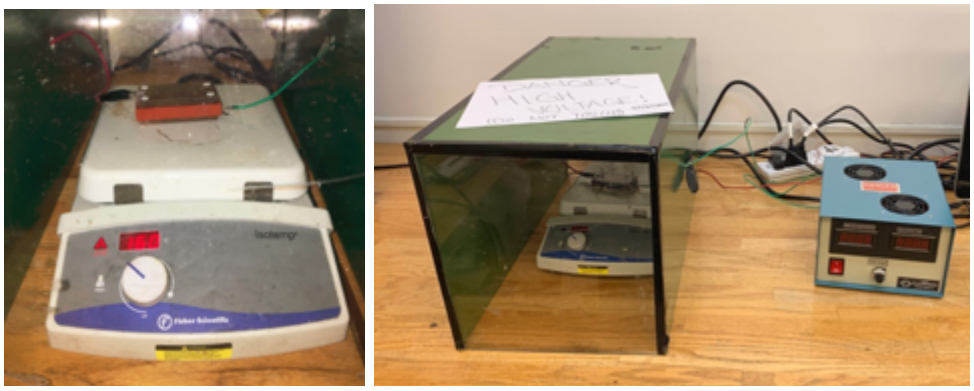

Figure 5-4 Device under poling conditions. Here, a porous sample is being poled at 150°C.

5.5. Electrical and Mechanical Testing of Samples

In order to determine the functionality of these devices, samples were repeatedly deformed while their electrical properties were evaluated. To achieve this, testing

apparatus were utilized. An amplifier magnifies the impulse data from a waveform generator. This is used to activate a shaker, which in turn moves the test stage up and down, effectively deforming the sample during testing. During this time, two electrodes connected to a data acquisition unit (DAQ) to collect electrical data and transmit it to the computer. Electrodes were placed on both the thin film and foam samples using adhesive copper tape. Due to the pores and lack of good contact, electrical tape was wrapped around the samples to make sure the electrodes stayed in place. Samples were repeatedly compressed, and their voltage recorded. This test set up is picture in Figure 5-5.

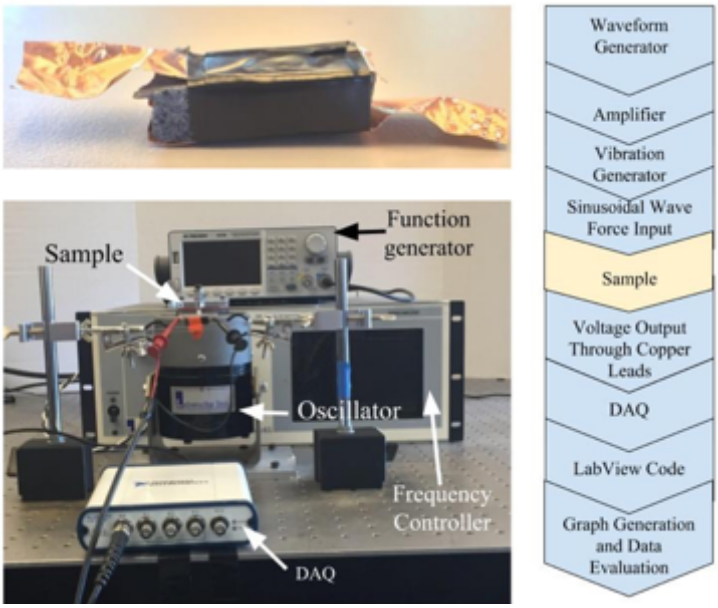

Figure 5-5 Electrical testing system for foamed samples.

The voltage from the device was forced through an electrical circuit. This circuit had a known resistance and the voltage across the resistor was collected. Then, using Ohm's law, the current is calculated.

Voltages were read and recorded at two locations, one at the device itself and one across a resistor. Voltage readings were gathered from the sample to get the direct voltage produced and across the resistor the voltage drop is measured to calculate the current output of the device. Figure 5-6 shows this electrical circuit and indicates where the measurements were taken during both testing set ups.

At first, several resistors were tested in order to determine which would provide the most consistent reading for electrical testing. Since the resistance of the sample changes as the sensor is deformed, large external resistors must be chosen to counter the changing sensor's piezoresistivity. Resistors at 1kΩ, 10kΩ, 100kΩ, and 1MΩ were chosen and ultimately, the largest size resistors, the 1MΩ resistors were used for testing.

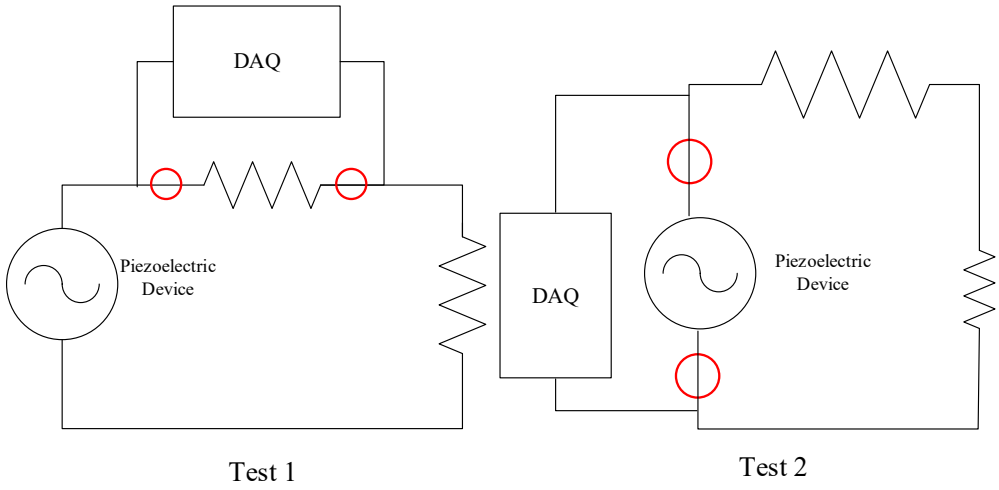

Figure 5-6 Piezoelectric testing system, red circle indicate were measurements were taken during either test. For test 1 the voltage drop across the resistor during compression can be used to calculate current. In test 2, the voltage output of the device is directly measured.

5.6. Thin film samples.

In Figure 5-7, an aligned thin film sample is compared to a sample that was not poled. The increased voltage output from the samples at 2 Hz is almost five times that of the unpoled samples, proving that dipole alignment could be achieved on thin film samples. The devices that underwent dipole alignment had a voltage output of 0.04V peak to peak (V_{pp}). The devices that did not undergo dipole alignment however only had a voltage output of 0.006 $V_{pp.}$

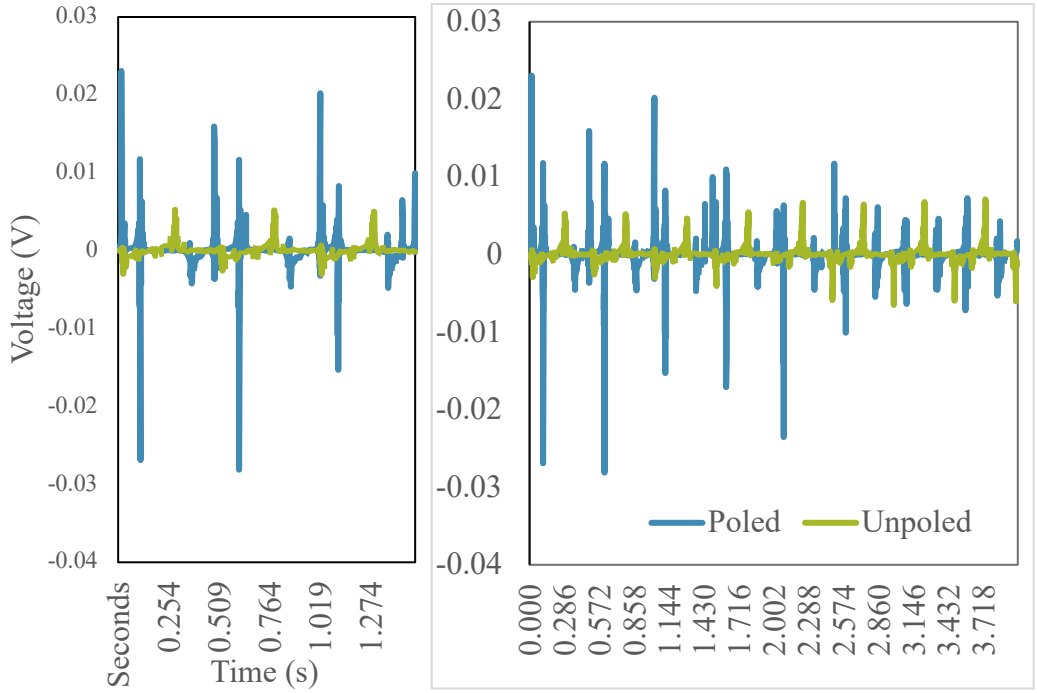

Figure 5-7 Voltage output of piezoelectric devices; left, 1.2 seconds, right, ~4 seconds).

Next, the sample's ability to produce a current was assessed. This is done by measuring the voltage across the resistor, as seen in Figure 5-6, where the DAQ recorded the voltage drop over a known resistor to calculate current. The results of these tests are seen in Figure 5-8. Here, the current output of the poled sample is 1.8× that of the unpoled sample. This clearly indicates successful alignment of dipoles and an increase the piezoelectric output of thin film devices. These results compare to what was achieved by other research groups like Yang et al. [13] where

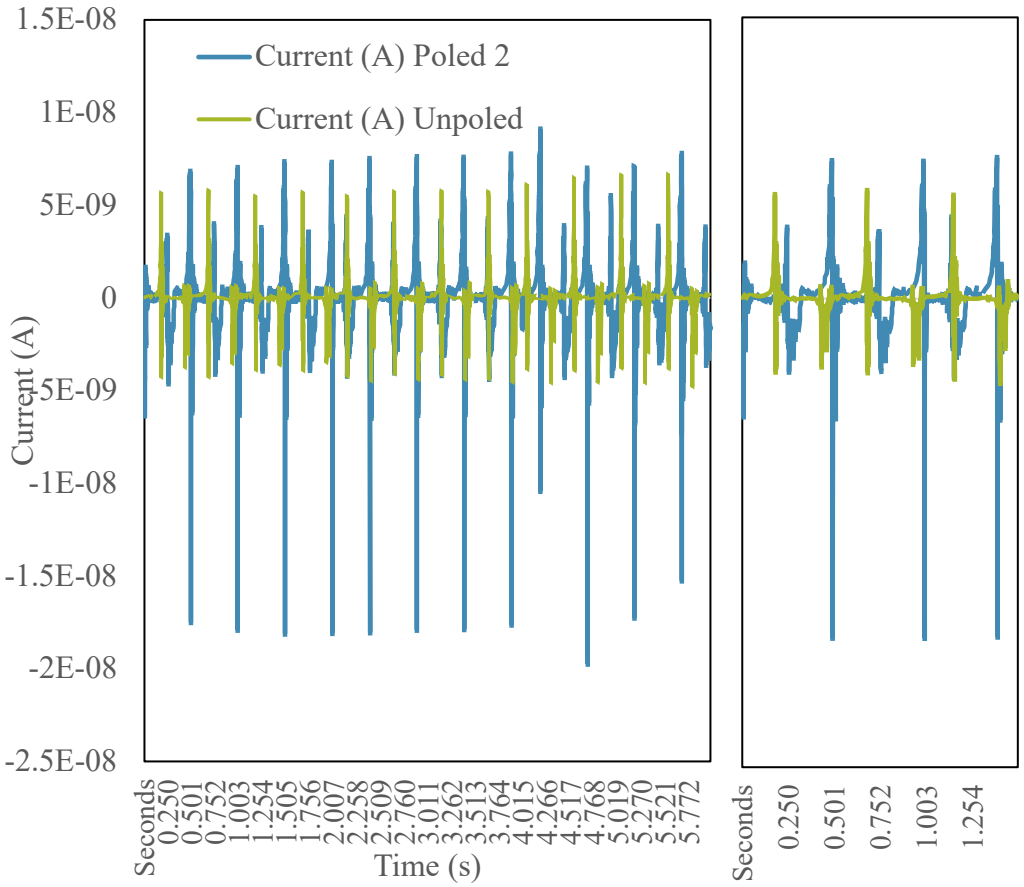

Figure 5-8 Current output of samples (6 second on left, 1.5 seconds on right).

5.7. Bulk samples.

When comparing the effects of dipole alignment on bulk samples, the increase in voltage output was not as successful as the thin film samples. All three different sugar samples, regardless of poling parameters, did not show the same significant increase in voltage output as poled vs. unpoled samples.

Some sugar/porosity configurations produced higher voltages, but not consistently. An example of a good voltage increase can be seen in Figure 5-9. As stated though, these results were inconsistent and is directly the cause for the research teams to visit the dispersion of nanomaterials when producing devices. The maximum peak to

peak voltage increases that were achievable with the bulk samples were with ultrafine, 60% sugar devices which produced 1.5× more voltage.

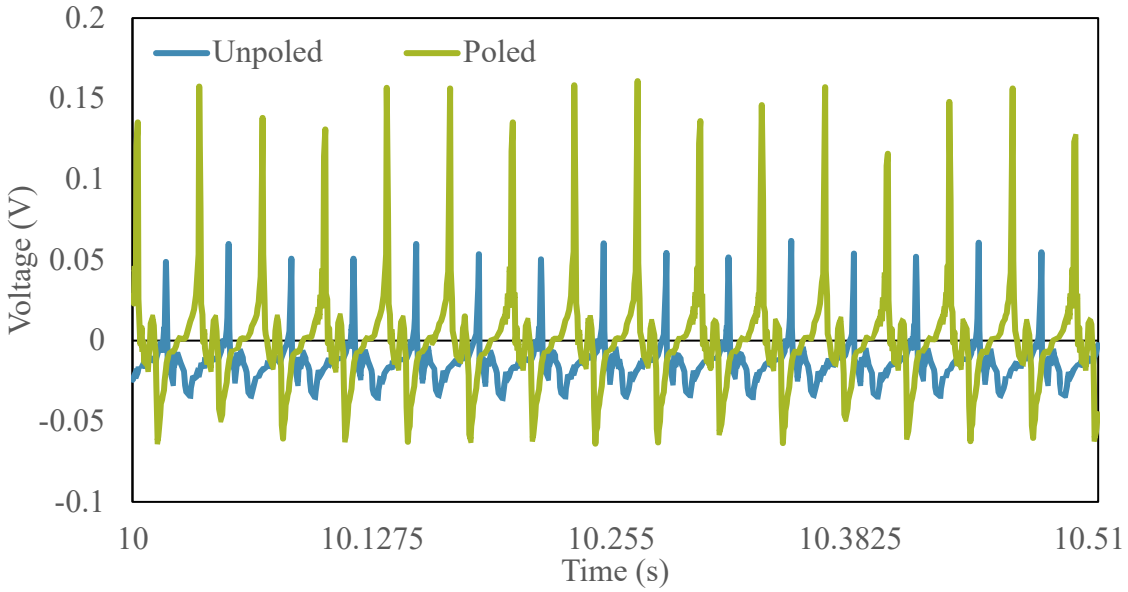

Figure 5-9 Ultrafine sugar, 60% porosity, poled vs. unpoled

This decrease in poling effectiveness is likely due to the thickness of the bulk samples during the dipole alignment process. The high voltages necessary to bridge the 10-12mm thick samples would cause dielectric breakdown in the nanocomposite. Therefore, voltages could not be set as high as what literature called for. To counter this, longer dipole alignment periods were tried. Samples were left for 12, 24, 48, and even once 72 hours to see if longer times would aid in alignment. All failed to provide the 10× increase in power output that was promised from the reading [18, 63]. Some however, did generate up to 1.8× the voltage output, although there was no change to current.

For these reasons, foamed energy harvesters were only a semi-successful endeavor in the scope of this project. Experiments were completed with the thin film

devices that were fabricated in literature and when the thin film samples were poled at significantly lower voltages, the process was successful. Devices had 5× the voltage output when poled. However, the bulk samples did not have the same success. Without a significant increase in current, the devices simply do not generate enough power to be used as energy harvesters. However, they still have applications as sensors.

Chapter 6

Conclusions and Future Works

6.1. Summary

In this paper, PDMS is functionalized with CNTs and ZnO to form nanocomposites in different applications. In order to produce well-dispersed nanocomposites, samples were produced using mechanical mixing and dispersion agents. Using SEM inspection, samples were imaged to determine the effectiveness of these mixing methods. The chloroform dispersion achieved more uniform dispersion than mechanical mixing. Because of this, chloroform dispersion was used for fabrication of most devices.

Next, porous samples were fabricated using different techniques. Ultimately, scaffolding with sugars was decided upon as the best method for producing porous devices. The sodium bicarbonate and the citric acid were both too dense and would sink to the bottom of the device before the device could cure, causing non-uniform pore distribution. While the layer of non-porous PDMS could be removed, this would alter the porosity of the sample. For this reason, the sugar samples that did not experience this separation layer (60%+ porosity) were the only ones considered for functionalization.

Porous structures were explored in order to determine which would have the optimal mechanical properties. The optimal configurations was the granulated sugar, 70% porosity. These samples had the most reliable mechanical properties during testing, making them dependable as sensors and possibly energy harvesters. This consistency is paramount to the predictability of a device's sensitivity; too much deviation in the Young's modulus of the devices would lead to varying sensitives between samples or the same type and therefore inconsistent data device to device.

Pressure sensing devices made with CNTs and PDMS were fabricated using a granulated sugar scaffold. Devices were fabricated using 70% scaffolding material and various amounts of CNTs to determine which would have the best sensitivity. The 3.5% CNT devices achieved this by having the lowest amount of CNTs a high conductivity during deformation. To be sure, samples were also fabricated using 0% (solid), 60%, 70% and 80% scaffolding material to see if porous structures effect sensitivity. As it were, the there is a slight reduction in the porous samples sensitivity, but they are still comparable. This means that despite this slight decrease in sensitivity, the cost reduction of materials by foaming devices is completely validated. Furthermore, the added ductility makes these devices applicable in situations where ergonomics or various stiffnesses could be beneficial. For example, in the bottom of a shoe for portable power or as subflooring in high-traffic areas to power lights.

Dipole alignment was a semi-successful endeavor. Researchers and laboratory experiments proved that with proper dispersion of nanomaterials and poling parameters, the piezoelectric effect of the devices could be amplified in the thin film devices. However, the bulk samples could not achieve the same increase due to their thickness.

6.2. Future Works

There are several aspects of this project that, given time, would have been worthwhile to investigate. These projects would have provided useful information that would further develop the results.

1.) During the compression of tactile sensors, the source meter and the SHIMPO machine could not communicate. Therefore, the pressure that was applied could not be recorded as the device was compressed. It was left to researchers

to look back on the source meter data and figure out what pressure was applied where. Therefore, samples had to be compressed at known intervals and pressures were superimposed over the change in resistance. Given time, a way to record both the actual pressure and the resistance at the same time would be beneficial for dynamic testing of pressure sensors in real-time. Real-time data would allow researchers to put the device under a cyclic load and study attributes like how quickly the sample responds, if there is any hysteresis, or if the rate at which pressure is applied affects the sensitivity.

2.) During the compression of tactile sensors, measurements began at 2 N to ensure a good connection between the foamed sample and the electrode. These devices had their most dramatic change in resistance between 2 and 4 N. Since the change in resistance between step increments keeps decreasing as more pressure is applied, it can comfortably be assumed that the samples would be even more sensitive in the 0-2 N range. However, starting at 0 N would mean that the electrode is not making contact with the foam sample, creating an open circuit with infinite resistance. The exponential decrease in resistance as the circuit is closed made it impossible to plot data for sensitivities in both 0 N and the 2-16 N range at the same time. Therefore, starting at a smaller pressure, perhaps 0.1 N, and using smaller increments, would ensure full contact with the sensor while also providing most of the data from the highly sensitive 0-2 N range.

3.) Given more time, the piezoelectric devices could be turned into energy harvesters. Unfortunately, due to time constraints, a further investigation of

foam piezoelectric dipole alignment was impossible. Given the time to explore dipole alignment further, more dependable piezoelectric devices could be produced. One thing that could possibly help is adding another dielectric layer to the poling device. When the bulk samples underwent dipole alignment, the foam and solid samples made direct contact with the copper plates, unlike with the thin film samples where a pure, non-conductive layer on PDMS was cast over the entire plate. This dielectric layer in the thin-film dipole alignment kept the system from shorting and causing dielectric breakdown. When the voltage was turned up on the bulk samples, this dielectric breakdown caused materials in the sample to carbonize and no longer function. Another suggestion is to try thinner bulk samples since thinner foam would require less voltage and possibly not cause dielectric breakdown. Data provided from these changes would further develop this project. If dipole alignment could consistently produce enough voltage for energy harvesting, the piezoelectric device could be used for more than just sensing.

4.) During the assessment of the devices, the voltage at the piezoelectric device could not be measured at the same time as the voltage drop across the resistor. Instead, researchers had to assume that the voltage produced at either location was unchanged while measurements were taken at the other location. In the future, researchers should try to create a system that can measure and record both sets of data simultaneously. By collecting data from both places at the same time, testing time would be cut in half. Further, if the DAQ could collect

both sets of data at the same time, researchers wouldn't need to assume the voltage remains unchanged during the two-part test.

5.) Currently, the nanocomposites function as non-implantable pressure sensors using either piezoresistivity or piezoelectricity. If developed fully, piezoresistive sensors could be used in dexterous robotics for tactile sensing. This would be accomplished by arranging multiple sensors into an array or into a humanoid arrangement like the one in Figure 1-1.

6.) The piezoelectric devices, once more developed could be used in energy harvesting applications. For example, harvesters on the bottom of shoes could charge a battery for portable power. Or, if the devices were scaled up, they could be used as subflooring in buildings. Foot traffic would cause deformations in the material and generate electricity. This would be especially useful in crowded places with heavy foot traffic like airports, stadiums, and malls. Long term, if these devices are developed fully, they could be used as bio-implantable energy harvesters and sensors for monitoring health and supplying power to implantable devices.

References

[1] K. S. Challagulla and T. A. Venkatesh, "Electromechanical response of piezoelectric foams," *Acta Materialia,* vol. 60, no. 5, pp. 2111-2127, 2012/03/01/ 2012.

[2] C. Liu, "Recent developments in polymer MEMS," *Advanced Materials,* vol. 19, no. 22, pp. 3783-3790, 2007.

[3] A. J. Bandodkar and J. Wang, "Non-invasive wearable electrochemical sensors: a review," *Trends in Biotechnology,* vol. 32, no. 7, pp. 363-371, 2014/07/01/ 2014.

[4] K. A. Cook-Chennault, N. Thambi, and A. M. Sastry, "Powering MEMS portable devices—a review of non-regenerative and regenerative power supply systems with special emphasis on piezoelectric energy harvesting systems," *Smart Materials and Structures,* vol. 17, no. 4, p. 043001, 2008.

[5] Metromatics, "Robotic Tactile Sensing," ed: Web3, 2019. <<https://metromatics.com.au/robotic-tactile-sensing/>>

[6] L. R. S. P.J. Sousa, L.M. Goncalves, G. Minas, "Patterned CNT-PDMS nanocomposites.pdf," 2015.

[7] K. Shin *et al.*, "Artificial Tactile Sensor Structure for Surface Topography Through Sliding," *IEEE/ASME Transactions on Mechatronics,* vol. 23, no. 6, pp. 2638-2649, 2018.

[8] G. Canavesea, S. Stassia,b, M. Strallac, C. Bignardic, C.F. Pirri, "Stretchable and Conformable Metal–Polymer Piezoresistive Hybrid System," *Sensors and Actuators A: Physical,* 2012.

[9] Z. Kappassov, J.-A. Corrales, and V. Perdereau, "Tactile sensing in dexterous robot hands — Review," *Robotics and Autonomous Systems,* vol. 74, pp. 195-220, 2015.

[10] J. I. Lee, S. Pyo, M. O. Kim, and J. Kim, "Multidirectional flexible force sensors based on confined, self-adjusting carbon nanotube arrays," *Nanotechnology,* vol. 29, no. 5, p. 055501, Feb 2 2018.

[11] C.-M. T. M. -Y. Cheng, Y.-Z. Lai, Y.-J. Yang, "The Development of a Highly Twistable Tactile Sensing Array," *Sensors and Actuators A: Physical,* 2009.

[12] C. Majidi, "Artificial Skin," 2016. *Soft Electronics & Sensors for Bio-Inspired Robots and Wearable Computing*

[13] X. Yang and W. A. Daoud, "Triboelectric and Piezoelectric Effects in a Combined Tribo-Piezoelectric Nanogenerator Based on an Interfacial ZnO Nanostructure," *Advanced Functional Materials,* vol. 26, no. 45, pp. 8194-8201, 2016.

[14] L. Dybowska-Sarapuk, J. Michalak, D. Janczak, J. Krzemiński, S. Lepak, and M. Jakubowska, *Sensors with potential application in artificial skin structure: review* (Photonics Applications in Astronomy, Communications, Industry, and High-Energy Physics Experiments 2018). SPIE, 2018.

[15] D. Zhou and H. Wang, "Design and evaluation of a skin-like sensor with high stretchability for contact pressure measurement," *Sensors and Actuators A: Physical,* vol. 204, pp. 114-121, 2013.

[16] J. Jordan, K. I. Jacob, R. Tannenbaum, M. A. Sharaf, and I. Jasiuk, "Experimental trends in polymer nanocomposites—a review," *Materials Science and Engineering: A,* vol. 393, no. 1, pp. 1-11, 2005/02/25/ 2005.

[17] H. Kim, A. A. Abdala, and C. W. Macosko, "Graphene/Polymer Nanocomposites," *Macromolecules,* vol. 43, no. 16, pp. 6515-6530, 2010/08/24 2010.

[18] N. Abinnas *et al.*, "0.8V nanogenerator for mechanical energy harvesting using bismuth titanate–PDMS nanocomposite," *Applied Surface Science,* vol. 418, pp. 362-368, 2017/10/01/ 2017.

[19] D. N. H. Tran, S. Kabiri, T. R. Sim, and D. Losic, "Selective adsorption of oil–water mixtures using polydimethylsiloxane (PDMS)–graphene sponges," *Environmental Science: Water Research & Technology,* vol. 1, no. 3, pp. 298-305, 2015.

[20] D. Zhu, S. Handschuh-Wang, and X. Zhou, "Recent progress in fabrication and application of polydimethylsiloxane sponges," *Journal of Materials Chemistry A,* 10.1039/C7TA04577H vol. 5, no. 32, pp. 16467-16497, 2017.

[21] (2019, May 20). *PDMS: A Review*. <<https://www.elveflow.com/microfluidic-tutorials/microfluidic-reviews-and-tutorials/the-poly-di-methyl-siloxane-pdms-and-microfluidics/>>

[22] K. I. Park *et al.*, "Flexible nanocomposite generator made of BaTiO(3) nanoparticles and graphitic carbons," *Adv Mater,* vol. 24, no. 22, pp. 2999-3004, 2937, Jun 12 2012.

[23] X. Gu, N. Li, H. Gu, X. Xia, and J. Xiong, "Polydimethylsiloxane-modified polyurethane–poly(ε-caprolactone) nanofibrous membranes for waterproof, breathable applications," *Journal of Applied Polymer Science,* vol. 135, no. 23, p. 46360, 2018/06/15 2018.

[24] S. Pyo *et al.*, "Development of a flexible three-axis tactile sensor based on screen-printed carbon nanotube-polymer composite," *Journal of Micromechanics and Microengineering,* vol. 24, no. 7, 2014.

[25] W. S. Lee, K. S. Yeo, A. Andriyana, Y. G. Shee, and F. R. Mahamd Adikan, "Effect of cyclic compression and curing agent concentration on the stabilization of mechanical properties of PDMS elastomer," *Materials & Design,* vol. 96, pp. 470-475, 2016/04/15/ 2016.

[26] M. Xie, K. Aw, B. Edwards, W. Gao, and P. Hu, "Orthogonal experimental design of polydimethylsiloxane curing for the design of low-frequency vibrational energy harvester," *Journal of Intelligent Material Systems and Structures,* vol. 25, no. 18, pp. 2228-2234, 2014.

[27] Giancarlo Canavesea, Stefano Stassia,b, Carmelo Fallautoc, Simone Corbellinic, and V. C. Valentina Caudaa, c, Marco Pirolac, Candido Fabrizio Pirria,b, "Piezoresistive Flexible Composite for Robotic Tactile Applications," *Sensors and Actuators A: Physical,* 2013.

[28] E. Hwang, J. Seo, and Y. Kim, "A Polymer-Based Flexible Tactile Sensor for Both Normal and Shear Load Detections and Its Application for Robotics," *Journal of Microelectromechanical Systems,* vol. 16, no. 3, pp. 556-563, 2007.

[29] S. Pyo *et al.*, "Batch fabricated flexible tactile sensor based on carbon nanotube-polymer composites," pp. 1004-1007: IEEE.

[30] C. Hu, W. Su, and W. Fang, "The integration of CNTs-based flexible tactile sensor and flexible circuit by polymer molding process," in *2011 16th International Solid-State Sensors, Actuators and Microsystems Conference*, 2011, pp. 414-417.

[31] W. O. a. T. Liu, "A Review: Carbon Nanotube-Based Piezoresistive Strain Sensors," *Journal of Sensors,* 2012.

[32] R. Ramalingame, N. Udhayakumar, R. Torres, I. T. Neckel, C. Müller, and O. Kanoun, "MWCNT-PDMS Nanocomposite Based Flexible Multifunctional Sensor for Health Monitoring," *Procedia Engineering,* vol. 168, pp. 1775-1778, 2016.

[33] G. Mittal, V. Dhand, K. Y. Rhee, S.-J. Park, and W. R. Lee, "A review on carbon nanotubes and graphene as fillers in reinforced polymer nanocomposites," *Journal of Industrial and Engineering Chemistry,* vol. 21, pp. 11-25, 2015/01/25/ 2015.

[34] L. J. Lee, C. Zeng, X. Cao, X. Han, J. Shen, and G. Xu, "Polymer nanocomposite foams," *Composites Science and Technology,* vol. 65, no. 15, pp. 2344-2363, 2005/12/01/ 2005.

[35] F. V. Ferreira *et al.*, *Functionalizing Graphene and Carbon Nanotubes: A Review* (no. Book, Whole). Cham: Springer International Publishing, 2016.

[36] D. Vairavapandian, P. Vichchulada, and M. D. Lay, "Preparation and modification of carbon nanotubes: Review of recent advances and applications in catalysis and sensing," *Analytica Chimica Acta,* vol. 626, no. 2, pp. 119-129, 2008/09/26/ 2008.

[37] M. Trojanowicz, "Analytical applications of carbon nanotubes: a review," *TrAC Trends in Analytical Chemistry,* vol. 25, no. 5, pp. 480-489, 2006/05/01/ 2006.

[38] I. V. Zaporotskova, N. P. Boroznina, Y. N. Parkhomenko, and L. V. Kozhitov, "Carbon nanotubes: Sensor properties. A review," *Modern Electronic Materials,* vol. 2, no. 4, pp. 95-105, 2016/12/01/ 2016.

[39] H. Birch, *50 Chemistry Ideas You Really Need to Know* (no. Generic). 2015.

[40] J. R. Sanchez-Valencia *et al.*, "Controlled synthesis of single-chirality carbon nanotubes," *Nature,* vol. 512, no. 7512, pp. 61-64, 2014.

[41] H. He, L. Ai Pham-Huy, P. Dramou, D. Xiao, P. Zuo, and C. Pham-Huy, *Carbon Nanotubes: Applications in Pharmacy and Medicine*. 2013, p. 578290.

[42] Y. Lai, Y. Chen, and Y. J. Yang, "A Novel CNT-PDMS-Based Tactile Sensing Array With Resistivity Retaining and Recovering by Using Dielectrophoresis Effect," *Journal of Microelectromechanical Systems,* vol. 21, no. 1, pp. 217-223, 2012.

[43] B. Safadi, R. Andrews, and E. A. Grulke, "Multiwalled carbon nanotube polymer composites: Synthesis and characterization of thin films," *Journal of Applied Polymer Science,* vol. 84, no. 14, pp. 2660-2669, 2002/06/28 2002.

[44] J.-i. Hahm, "Fundamental Properties of One-Dimensional Zinc Oxide Nanomaterials and Implementations in Various Detection Modes of Enhanced Biosensing," *Annual Review of Physical Chemistry,* vol. 67, no. 1, pp. 691-717, 2016/05/27 2016.

[45] A. Sirelkhatim *et al.*, "Review on Zinc Oxide Nanoparticles: Antibacterial Activity and Toxicity Mechanism," *Nano-Micro Letters,* vol. 7, no. 3, pp. 219-242, 2015/07/01 2015.

[46] J. S. Dodds, F. N. Meyers, and K. J. Loh, "Piezoelectric Characterization of PVDF-TrFE Thin Films Enhanced With ZnO Nanoparticles," *IEEE Sensors Journal,* vol. 12, no. 6, pp. 1889-1890, 2012.

[47] J. S. Dodds, F. N. Meyers, and K. J. Loh, "Enhancing the piezoelectric performance of PVDF-TrFE thin films using zinc oxide nanoparticles," vol. 8345, pp. 834515-834519: SPIE.

[48] C. X. Liu and J. W. Choi, "Improved Dispersion of Carbon Nanotubes in Polymers at High Concentrations," *Nanomaterials (Basel),* vol. 2, no. 4, pp. 329-347, Oct 26 2012.

[49] J. H. Kim *et al.*, "Simple and cost-effective method of highly conductive and elastic carbon nanotube/polydimethylsiloxane composite for wearable electronics," (in English), *Scientific Reports (Nature Publisher Group),* vol. 8, pp. 1-11, Jan 2018

[50] R. Zargar, J. Nourmohammadi, and G. Amoabediny, "Preparation, characterization, and silanization of 3D microporous PDMS structure with properly sized pores for endothelial cell culture," *Biotechnology and Applied Biochemistry,* vol. 63, no. 2, pp. 190-199, 2016/03/01 2015.

[51] Q. Li *et al.*, "Engineering of carbon nanotube/polydimethylsiloxane nanocomposites with enhanced sensitivity for wearable motion sensors," *Journal of Materials Chemistry C,* 10.1039/C7TC03434B vol. 5, no. 42, pp. 11092-11099, 2017.

[52] L. Zhu, Y. Wang, D. Mei, and X. Wu, "Highly Sensitive and Flexible Tactile Sensor Based on Porous Graphene Sponges for Distributed Tactile Sensing in Monitoring Human Motions," *Journal of Microelectromechanical Systems,* vol. 28, no. 1, pp. 154-163, 2019.

[53] P. X. Ma, "Scaffolds for tissue fabrication," *Materials Today,* vol. 7, no. 5, pp. 30-40, 2004/05/01/ 2004.

[54] J. L. Ruiz-Herrero, M. A. Rodríguez-Pérez, and J. A. de Saja, "Effective diffusion coefficient for the gas contained in closed cell polyethylene-based foams subjected to compressive creep tests," *Polymer,* vol. 46, no. 9, pp. 3105-3110, 2005/04/15/ 2005.

[55] J. Chruściel Jerzy and E. Leśniak, "Preparation of flexible, self-extinguishing silicone foams," *Journal of Applied Polymer Science,* vol. 119, no. 3, pp. 1696-1703, 2011/02/05 2010.

[56] S. C. Frerich, "Biopolymer foaming with supercritical CO2—Thermodynamics, foaming behaviour and mechanical characteristics," *The Journal of Supercritical Fluids,* vol. 96, pp. 349-358, 2015/01/01/ 2015.

[57] A. S. Dutta, "2 - Polyurethane Foam Chemistry," in *Recycling of Polyurethane Foams*, S. Thomas, A. V. Rane, K. Kanny, A. V.K, and M. G. Thomas, Eds.: William Andrew Publishing, 2018, pp. 17-27.

[58] M. Emami, R. Thompson Michael, and J. Vlachopoulos, "Bubble nucleation in nonpressurized polymer foaming systems," *Polymer Engineering & Science,* vol. 54, no. 5, pp. 1201-1210, 2014/05/01 2013.

[59] A. Menner and A. Bismarck, "New Evidence for the Mechanism of the Pore Formation in Polymerising High Internal Phase Emulsions or Why polyHIPEs Have an Interconnected Pore Network Structure," *Macromolecular Symposia,* vol. 242, no. 1, pp. 19-24, 2006/10/01 2006.

[60] J. E. Dusek, M. S. Triantafyllou, and J. H. Lang, "Piezoresistive foam sensor arrays for marine applications," *Sensors and Actuators A: Physical,* vol. 248, pp. 173-183, 2016/09/01/ 2016.

[61] (2019, April 11). *Pressure-Sensitive Conductive Sheet (Velostat/Linqstat)*.

[62] G. Zhu *et al.*, "Toward Large-Scale Energy Harvesting by a Nanoparticle-Enhanced Triboelectric Nanogenerator," *Nano Letters,* vol. 13, no. 2, pp. 847-853, 2013/02/13 2013.

[63] H. m Sun *et al.*, "A novel flexible nanogenerator made of ZnO nanoparticles and multiwall carbon nanotube," *Nanoscale,* 10.1039/C3NR00866E vol. 5, no. 13, pp. 6117-6123, 2013.

[64] C. Dagdeviren *et al.*, "Transient, Biocompatible Electronics and Energy Harvesters Based on ZnO," *Small,* vol. 9, no. 20, pp. 3398-3404, 2013.

[65] S. Saadon and O. Sidek, "A review of vibration-based MEMS piezoelectric energy harvesters," *Energy Conversion and Management,* vol. 52, no. 1, pp. 500-504, 2011/01/01/ 2011.

[66] J. S. Dodds, "Development of Piezoelectric Zinc Oxide Nanoparticle-Poly(Vinylidene Fluoride) Nanocomposites for Sensing and Actuation," Dissertation/Thesis, ProQuest Dissertations Publishing, 2013.

[67] L. Jiang *et al.*, "Flexible piezoelectric ultrasonic energy harvester array for bio-implantable wireless generator," *Nano Energy,* vol. 56, pp. 216-224, 2019/02/01/ 2019.

[68] A. D. Prewitt, "Effects of the poling process on dielectric, piezoelectric, and ferroelectric properties of lead zirconate titanate.," 2012.

[69] S. Tadigadapa and K. Mateti, "Piezoelectric MEMS sensors: state-of-the-art and perspectives," *Measurement Science and Technology,* vol. 20, no. 9, p. 092001, 2009/07/24 2009.

[70] K. I. Park, C. K. Jeong, J. Ryu, G. T. Hwang, and K. J. Lee, "Flexible and Large-Area Nanocomposite Generators Based on Lead Zirconate Titanate Particles and Carbon Nanotubes," *Advanced Energy Materials,* vol. 3, no. 12, pp. 1539-1544, 2013.

[71] C. K. Jeong, K.-I. Park, J. Ryu, G.-T. Hwang, and K. J. Lee, "Large-Area and Flexible Lead-Free Nanocomposite Generator Using Alkaline Niobate Particles and Metal Nanorod Filler," *Advanced Functional Materials,* vol. 24, no. 18, pp. 2620-2629, 2014.

[72] P. Yi, R. A. Awang, W. S. T. Rowe, K. Kalantar-zadeh, and K. Khoshmanesh, "PDMS nanocomposites for heat transfer enhancement in microfluidic platforms," *Lab on a Chip,* 10.1039/C4LC00615A vol. 14, no. 17, pp. 3419-3426, 2014.

[73] V. Silverio, A. V. Silva, K. Przykaza, L. F. Santos, L. V. Melo, and S. Cardoso, "Dark matters: black-PDMS nanocomposite for opaque microfluidic systems," *Physical Chemistry Chemical Physics,* 10.1039/C8CP06828C vol. 21, no. 5, pp. 2719-2726, 2019.

[74] X. Liu *et al.*, "Direct synthesis of mesoporous Fe3O4 through citric acid-assisted solid thermal decomposition," *Journal of Materials Science,* journal article vol. 45, no. 4, p. 906, November 17 2009.